PECTIN ACETYLESTERASE9 Affects the Transcriptome and Metabolome and Delays Aphid Feeding[1][OPEN]

Karen J. Kloth,[a,b,2] Ilka N. Abreu,[c] Nicolas Delhomme,[c] Ivan Petřík,[d,e] Cloé Villard,[f] Cecilia Ström,[a] Fariba Amini,[a,g] Ondřej Novák,[c,d] Thomas Moritz,[c] and Benedicte R. Albrectsen[a,3]

[a]Department of Plant Physiology, Umeå Plant Science Centre, Umeå University, S-90187 Umea, Sweden
[b]Laboratory of Entomology, Wageningen University and Research, 6700 AA Wageningen, The Netherlands
[c]Department of Forest Genetics and Physiology, Umeå Plant Science Centre, Swedish Agriculture University, S-90183 Umea, Sweden
[d]Laboratory of Growth Regulators, Centre of the Region Haná for Biotechnological and Agricultural Research, Institute of Experimental Botany CAS and Faculty of Science of Palacký University, Šlechtitelů 27, CZ-78371 Olomouc, Czech Republic
[e]Department of Chemical Biology and Genetics, Centre of the Region Haná for Biotechnological and Agricultural Research, Faculty of Science, Palacký University, Šlechtitelů 27, CZ-78371 Olomouc, Czech Republic
[f]Unité de recherche Inserm 1121, Université de Lorraine-INRA Laboratoire Agronomie et Environnement ENSAIA, 2 Avenue Forêt de Haye, 54518 Vandœuvre-lès-Nancy, France
[g]Department of Biology, Faculty of Science, Arak University, Arak 38156-8-8349, Iran

ORCID IDs: 0000-0002-0379-5473 (K.J.K.); 0000-0003-4728-0161 (I.N.A.); 0000-0002-3053-0796 (N.D.); 0000-0002-4258-3190 (T.M.); 0000-0002-9337-4540 (B.R.A.).

The plant cell wall plays an important role in damage-associated molecular pattern–induced resistance to pathogens and herbivorous insects. Our current understanding of cell wall-mediated resistance is largely based on the degree of pectin methylesterification. However, little is known about the role of pectin acetylesterification in plant immunity. This study describes how one pectin-modifying enzyme, *PECTIN ACETYLESTERASE 9* (*PAE9*), affects the Arabidopsis (*Arabidopsis thaliana*) transcriptome, secondary metabolome, and aphid performance. Electro-penetration graphs showed that *Myzus persicae* aphids established phloem feeding earlier on *pae9* mutants. Whole-genome transcriptome analysis revealed a set of 56 differentially expressed genes (DEGs) between uninfested *pae9-2* mutants and wild-type plants. The majority of the DEGs were enriched for biotic stress responses and down-regulated in the *pae9-2* mutant, including *PAD3* and *IGMT2*, involved in camalexin and indole glucosinolate biosynthesis, respectively. Relative quantification of more than 100 secondary metabolites revealed decreased levels of several compounds, including camalexin and oxylipins, in two independent *pae9* mutants. In addition, absolute quantification of phytohormones showed that jasmonic acid (JA), jasmonoyl-Ile, salicylic acid, abscisic acid, and indole-3-acetic acid were compromised due to PAE9 loss of function. After aphid infestation, however, *pae9* mutants increased their levels of camalexin, glucosinolates, and JA, and no long-term effects were observed on aphid fitness. Overall, these data show that PAE9 is required for constitutive up-regulation of defense-related compounds, but that it is not required for aphid-induced defenses. The signatures of phenolic antioxidants, phytoprostanes, and oxidative stress–related transcripts indicate that the processes underlying PAE9 activity involve oxidation-reduction reactions.

The ability to sense and respond to danger is a fundamental aspect for living beings across kingdoms (Matzinger, 1994; Matzinger, 2002). In plants, the primary cell wall plays a central role in protecting against attacks by pathogens and herbivores. The matrix of cellulose and hemicellulose fibrils and pectin forms a physical barrier and requires invaders to secrete digestive enzymes or to use mechanical force for breaching it (Albersheim et al., 1969). Apart from that, the cell wall plays a prominent role in sensing and signaling of biotic stress. A wide range of receptors and sensors on the plasma membrane can recognize infections in the apoplast and trigger a cascade of immune responses in the symplast (Delaunois et al., 2014; Wolf, 2017). Elicitors that bind to cell wall–associated receptors are not only pathogen-associated molecular patterns or herbivore-associated molecular patterns, such as chitin (Zipfel et al., 2004; Wu and Baldwin, 2010), but also 'self-damage' particles from the plant, called damage-associated molecular patterns (DAMPs; Ferrari et al., 2013; Heil and Land, 2014). DAMPs can be induced by pathogens and herbivores via mechanical damage or the secretion of lytic enzymes (Vorhölter et al., 2012), but they can also be suppressed via the secretion of effectors (Huang et al., 2019).

DAMPs can consist of a variety of molecules, for example extracellular DNA fragments, misfolded proteins, or cell wall–derived molecules (Lotze et al., 2007).

Not surprisingly, many characterized DAMPs originate from pectin, the most abundant primary cell wall polysaccharide in nongraminaceous plants consisting of a homogalacturonan or rhamnogalacturonan backbone (Creelman and Mullet, 1997; Ridley et al., 2001; Caffall and Mohnen, 2009). Fragmented pectin polymers, referred to as oligogalacturonides (OGs), are important inducers of the salicylic acid (SA) and jasmonic acid (JA) pathway, reactive oxygen species (ROS), and antimicrobial phytoalexins (Hahn et al., 1981; Davis et al., 1986; Shaw and Long, 2003; Vorwerk et al., 2004; Bethke et al., 2016; Bacete et al., 2018). Wall-associated kinases (WAKs) play an important role in DAMP-induced responses and cell wall integrity signaling (Brutus et al., 2010; De Lorenzo et al., 2011; Novaković et al., 2018).

Interestingly, the elicitor capacity of pectin fragments is largely determined by the organization and abundance of methyl and acetyl moieties on the pectin backbone. Pectins are synthesized in the Golgi apparatus and densely decorated with methyl and acetyl groups (Cosgrove, 2005; Levesque-Tremblay et al., 2015). After secretion into the apoplast, plant-derived pectinesterases remove methyl or acetyl groups in muro via pectin methylesterases (PMEs) and pectin acetylesterases (PAEs). When deesterification occurs in block-wise patterns, pectin polymers tend to ionically cross-link to one another in the presence of cations, such as Ca^{2+}, to produce so called 'egg-box' formations (Liners et al., 1989; Jarvis and Apperley, 1995).

Current insights in the effects of pectin deesterification on plant resistance are mostly based on pectin demethylation (Levesque-Tremblay et al., 2015), and these insights seem to be varied and often antagonistic (Fig. 1). Although block-wise deesterification makes pectin more prone to egg-box formation and increases gel stability and cell wall stiffness (Willats et al., 2001; Cosgrove, 2005; Caffall and Mohnen, 2009; Bidhendi and Geitmann, 2016), the pectin backbone simultaneously becomes more exposed to plant- or pathogen-derived pectin-degrading enzymes (Biely et al., 1986; McMillan et al., 1993; Pelloux et al., 2007; Raiola et al., 2011; Bi et al., 2016; Lionetti et al., 2017). This increases risks for pathogenic intrusion, but simultaneously leads to the accumulation of more OGs and thus enhances DAMP-induced responses (Pogorelko et al., 2013a; Bethke et al., 2014). Moreover, OGs from deesterified pectin tend to have a higher binding efficiency to WAKs due to reduced polymer size and egg-box configurations, and can thereby induce stronger cell wall integrity signals (Decreux and Messiaen, 2005; Cabrera et al., 2008; Osorio et al., 2008; Kohorn et al., 2014).

Other expected consequences of pectin deesterification include the release of free methanol or acetate that can be reincorporated in plant metabolism. Negatively charged carboxyl groups will accumulate, causing a hypothetical pH drop with unknown effects, for example wall-loosening actions by expansins, and the function of other apoplastic proteins and ion channels (Aldington et al., 1991; Pelloux et al., 2007; Cosgrove, 2015). A still understudied component of pectin deesterification is the potential consequences for the apoplastic homeostasis in ROS, as ROS are catabolized during the process of cell wall cross-linking and loosening (Cosgrove, 2005; Kärkönen and Kuchitsu, 2015; Schmidt et al., 2016). Overall, independent studies have shown that pectin configurations play an important role in plant immunity against biotrophic and necrotrophic pathogens and provide new opportunities for sustainable pest and disease management (De Lorenzo et al., 2011; Pogorelko et al., 2013b; Bethke et al., 2016; Bacete et al., 2018). Current understandings of cell wall-mediated immunity and its downstream effects on the plant transcriptome and metabolome are, however, limited and mostly based on pectin demethylation.

Here, we studied the role of the Arabidopsis (*Arabidopsis thaliana*) PECTIN ACETYLESTERASE 9 (PAE9) in plant secondary metabolism and resistance to an important insect pest, *Myzus persicae* aphids (Blackman and Eastop, 2006). Arabidopsis has 12 PAEs, of which PAE9 is more distantly related to the other PAEs and occurs in several monocot and dicot families (Philippe et al., 2017). de Souza et al. (2014) found that the preferred substrate of PAE9 is the pectic polysaccharide rhamnogalacturonan I, and potentially also homogalacturonan, and that *pae9-1* and *pae9-2* mutants have 15% to 20% more pectin acetylation. As PAE9 is nonredundant and has no apparent plant growth phenotype (de Souza et al., 2014), we selected this deacetylation enzyme to investigate its potential role in plant resistance to aphids.

Plant resistance can be distinguished in two main categories: constitutive resistance, where plants possess by default one or more traits that improve plant fitness by impairing pathogen or herbivore performance, and

[1]This work was supported by Carl Tryggers Stiftelse för Vetenskaplig Forskning (CTS15:14), the Knut and Alice Wallenberg Foundation via the Kungliga Skogsoch Lantbruksakademien (GFS2016:0019), Bio4Energy (Swedish Programme for Renewable Energy), Vinnova (the Swedish Governmental Agency for Innovation Systems), and KAW (The Knut and Alice Wallenberg Foundation). Phytohormone measurements were supported by the Ministry of Education, Youth and Sports of the Czech Republic through the European Regional Development Fund-Project 'Centre for Experimental Plant Biology' (CZ.02.1.01/0.0/0.0/16_019/0000738) and the Internal Grant Agency of Palacký University (project no. IGA_PrF_2019_020).

[2]Author for contact: karen.kloth@wur.nl.

[3]Senior author.

The author responsible for distribution of materials integral to the findings presented in this article in accordance with the policy described in the Instructions for Authors (www.plantphysiol.org) is: Karen J. Kloth (karen.kloth@wur.nl).

K.J.K. and B.R.A. conceived the original screening and research plans, and wrote the article with contributions of all the authors; K.J.K. designed the experiments and analyzed the data; I.N.A. and I.P. performed the metabolomic analyses; N.D. supervised the transcriptomic analyses; C.V., C.S., and F.A. provided technical assistance in data collection; C.S. performed cryofixation and microscopy; O.N. and T.M. supervised the metabolomic analyses.

[OPEN]Articles can be viewed without a subscription.

www.plantphysiol.org/cgi/doi/10.1104/pp.19.00635

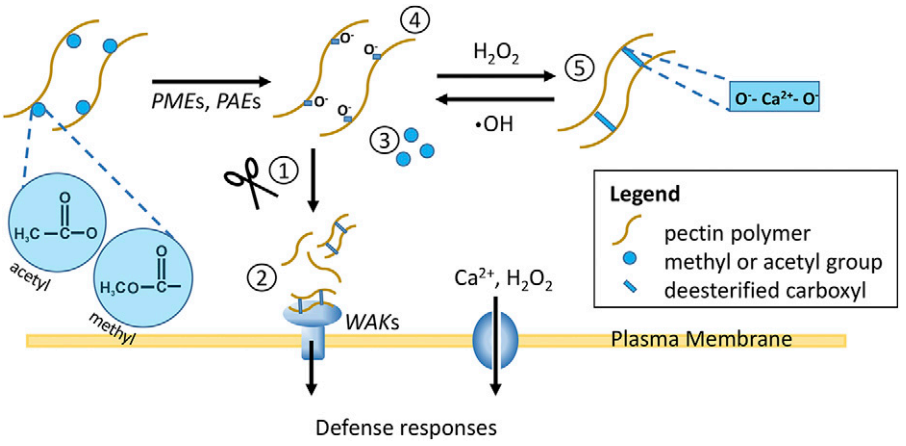

Figure 1. Hypothetical effects of PMEs and PAEs on plant resistance: (1) Increased accessibility for pectin degrading enzymes, (2) production of more, smaller, and cross-linked OGs (DAMPs) that bind to WAKs and induce defense responses, (3) the release of free methanol or acetate that can be reincorporated in primary and secondary metabolism, (4) more negatively charged carboxyl groups that decrease the pH of the apoplast, and (5) more ROS-mediated pectin cross-linking with potential effects on ROS and calcium influxes into the cell.

induced resistance, where plants mount a response against their attackers only after damage, infection, or infestation has occurred (Schoonhoven et al., 2005). Aphids are phloem-feeding insects that have intense contact with the cell wall. They generally do not damage cells, but maneuver their telescoping piercing-sucking stylet mouth through the cell wall matrix (Fig. 2). They briefly puncture cells along their path and ingest small amounts of cell content. Eventually they aim to find a sieve tube where they can feed from the phloem sap (Tjallingii and Hogen Esch, 1993).

Cell wall penetration may take several hours and is accompanied by the secretion of gelling saliva. This is considered to be another class of saliva than the 'watery' saliva, which is secreted in the sieve tube before and during sap ingestion (Mutti et al., 2008; Rodriguez and Bos, 2013; van Bel and Will, 2016). Aphid saliva contains effectors, such as calcium-binding proteins, that are considered to counteract defense responses in the phloem, and, depending on the aphid species, pectin-modifying enzymes, such as polygalacturonases and pectinesterases (Dreyer and Campbell, 1987; Ma et al., 1990; Miles, 1999; Cherqui and Tjallingii, 2000; van Bel and Will, 2016; Kloth et al., 2017). A recent study showed that *M. persicae* aphids benefit from PME activity, potentially due to increased flexibility of the cell wall, but also due to unknown factors in the phloem (Silva-Sanzana et al., 2019). The latter illustrates that, apart from being a constitutive physical barrier to aphids, the cell wall is involved in induced plant responses and systemic changes. This is accompanied by transcriptional evidence that aphids affect the expression of many cell wall–modifying genes (Divol et al., 2007; Smith and Boyko, 2007; De Vos and Jander, 2009) and induce WAKs (Kuśnierczyk et al., 2008; Foyer et al., 2015; Kloth et al., 2016).

In our study, we hypothesized that PAE9 activity would, on the one hand, facilitate cell wall penetration by *M. persicae* aphids, as deacetylated pectin would be more vulnerable for breakdown by aphid effectors. On the other hand, we expected PAE9 to enhance DAMP-induced defenses against aphids. Our results illustrate that PAE9 increases biotic stress-related transcription and secondary metabolism, as shown by higher levels of, for example, JA, camalexin, and antioxidants in uninfested plants, but that PAE9 is not required for aphid-induced up-regulation of these defense compounds.

RESULTS

PAE9 Reduces Aphid Feeding But Not Aphid Fitness

To study the effects of PAE9 (*AT5G23870*) on *M. persicae*, homozygous Arabidopsis Transfer-DNA (T-DNA) insertion mutants *pae9-1* and *pae9-2* were selected and

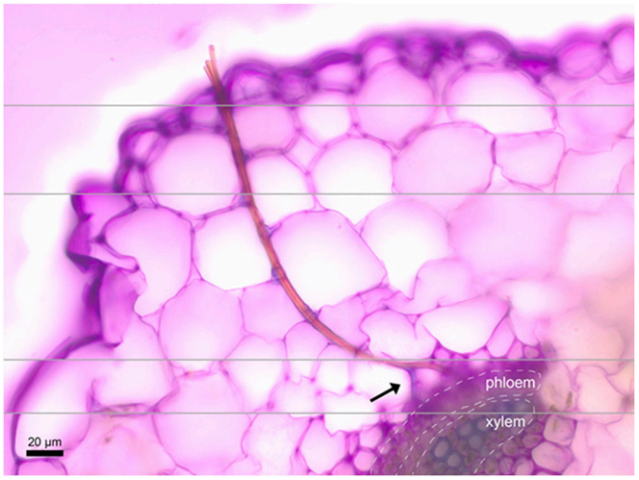

Figure 2. Cryofixed *M. persicae* aphid stylets in an Arabidopsis leaf. The stylet position illustrates the intimate contact between an aphid and the plant cell wall. Aphids usually do not disrupt cells, but maneuver their stylets through the apoplast and sample several cells along their way to the phloem. Cell wall penetration can take between 10 min and several hours and is accompanied by the secretion of gelling saliva. After arrival at a sieve tube, aphids start phloem feeding and usually keep their stylets anchored for hours or even days. This aphid reached the phloem in 15 min, after penetrating along a track of at least 26 μm of cell wall (not accounting for movements in the direction of the z plane) and showing 25 brief plasma membrane punctures along its path. The arrow indicates an abandoned tract with remnants of gelling saliva (toluidine blue staining, images of different depth of focus are separated with gray lines).

validated for abolished gene expression (Supplemental Fig. S1). de Souza et al. (2014) had shown that these loss-of-function mutants contained 15% to 20% more pectin acetylation compared with the wild type, Columbia (Col-0). These genotypes were subsequently screened for aphid feeding behavior by electrical penetration graph (EPG) recording. This technique uses aphids as bio-electrodes in a low-voltage electrical circuit. From the recorded electrical patterns, stylet activities, such as penetration of the epidermis and mesophyll, salivation in the phloem, and phloem feeding were annotated (Tjallingii, 1988). Aphid feeding behavior was monitored with EPG recording on 5-week-old plants for 8 h. Overall probing behavior summarized over the 8-h recording duration did not reveal any effects. A more or less comparable proportion of the aphids (25% on wild type, 14% on the *pae9* mutants) encountered penetration difficulties in the cell wall (Supplemental Table S1). In addition, the residence of the aphid stylets in the cell wall and its latency to the first arrival at a sieve tube was not significantly different. The aphid stylets arrived at a comparable rate at the sieve elements and spent comparable total amounts of time in the epidermis, mesophyll, and sieve elements (Supplemental Table S1). Time trends revealed, however, a distinctive pattern inside the sieve tubes. After the first 4 h of settling, aphids established phloem feeding earlier in the mutants and showed more nonprobing activities in the wild type (Fig. 3A). Also, the proportion of time spent on the secretion of saliva in the phloem phase was smaller on the *pae9-1* mutant ($P < 0.05$, $n = 14$, Supplemental Tables S1 and S2), implying that there was less need for the secretion of effectors in the phloem sap.

As these observations pointed toward a sieve tube-located resistance effect of PAE9 on *M. persicae* aphids, the impact on aphid fitness was measured. Three-week-old plants of a similar development stage (10–12 leaves) were infested with one neonate aphid each. Previously, we had seen that uninfested rosettes were of similar biomass (Col-0 1.1 ± 0.1, *pae9-1* 1.3 ± 0.1, *pae9-2* 1.0 ± 0.1 g fresh weight, $P > 0.05$, $n = 10$, 6-week-old plants). However, after the 2-week infestation we observed a decline in rosette biomass in the *pae9* mutants (Fig. 3B) and a positive correlation between rosette fresh weight and aphid numbers ($P = 0.04$, Pearson, one-sided $r^2 = 0.09$). Aphid fitness was therefore corrected for plant biomass in a mixed

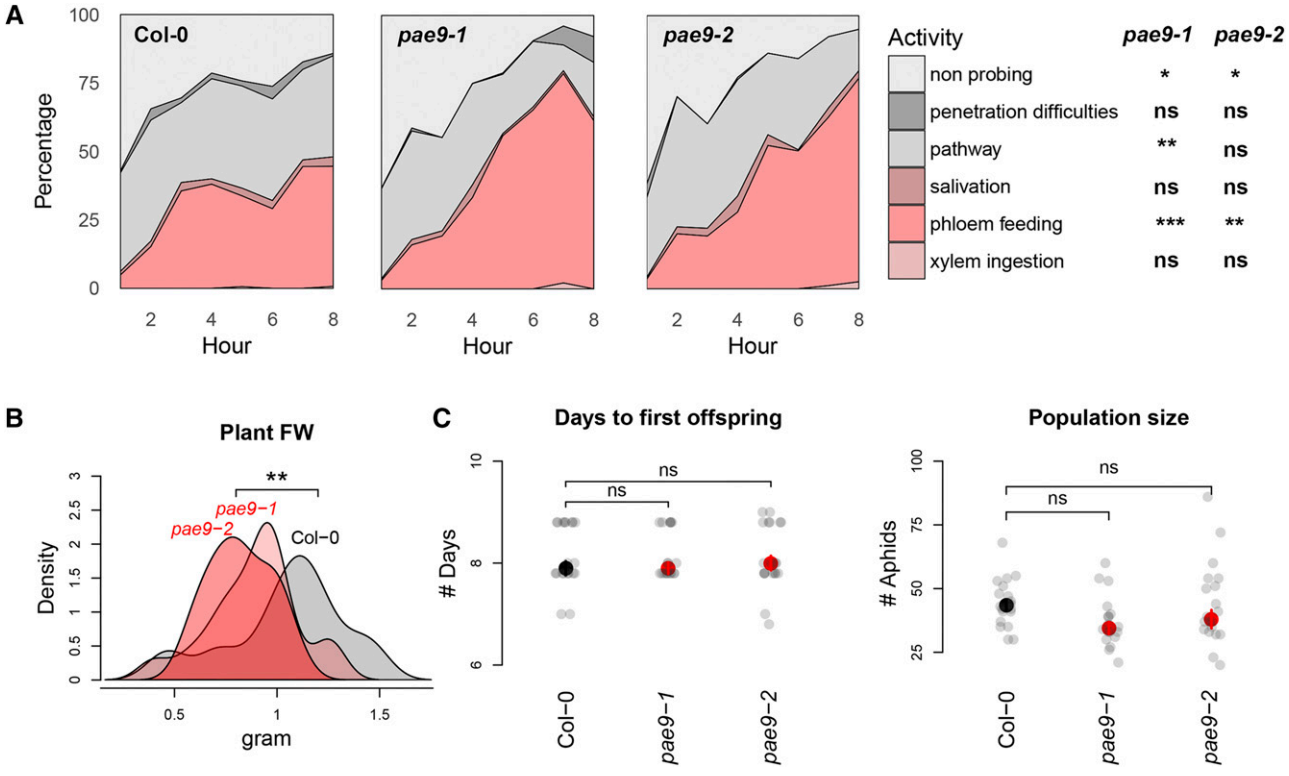

Figure 3. Effects of *pae9-2* mutants on *M. persicae* aphids. A, Aphid feeding behavior during 8-h EPG recordings, expressed as the mean percentage of time per hour ('pathway' = cell wall penetration phase, significance of plant line × time interactions in linear mixed model: $*P < 0.05$, $**P < 0.01$, $***P < 0.001$, $n = 14$, for Col-0 the mean of two experiments is depicted; ns, not significant). B, Plant fresh weight (FW; density diagram, $P = 0.0091$, $n = 20$, one-way ANOVA). C, Aphid development time from neonate to adult and aphid population sizes after 2 weeks of infestation with one neonate ($P = 0.07$, $P = 0.68$, $n = 20$, mixed linear model with plant fresh weight as random effect). Gray dots represent individual data points, red or black dots represent the mean value, and the error bar the 95% confidence interval.

model. This showed that nymphs developed into adults at a comparable developmental rate on *pae9* and wild-type plants and eventually produced comparable amounts of offspring, although we observed a nonsignificant trend of lower aphid numbers on the *pae9-1* mutant ($P = 0.07$, $n = 20$), which was not confirmed on the *pae9-2* mutant ($P = 0.68$, $n = 20$, Fig. 3C). Based on these observations on aphid behavior in the first 8 h of host contact and aphid reproduction over a 2-week time frame, we hypothesized that PAE9 may increase constitutive but not aphid-induced plant resistance.

Constitutively Down-Regulated Biotic Stress-Related Genes in the *pae9-2* Mutant

To study the effect of PAE9 before and after aphid infestation, RNA sequencing (RNA-Seq) was performed on wild-type and *pae9-2* plants. Plants were subjected to either of the following treatments: (1) no aphids (control), (2) 4 h postinfestation (hpi) with 20 aphids per plant, and (3) 8 hpi with 20 aphids per plant. RNA-Seq libraries were made of three biological replicates and sequenced with Illumina technology. Between 10 and 16 million raw 126 bp paired-end reads were generated per sample, of which more than 90% mapped to unique loci on the Arabidopsis reference transcriptome, monitoring the expression of 25,538 genes (Supplemental Table S3). In total, 56 genes were differentially expressed between *pae9-2* and Col-0 plants in the control treatment, 44 at 4 hpi, and 14 at 8 hpi (adjusted $P <= 0.01$, log fold change $\geq$ 0.5, Supplemental Table S4). Around 25% of the differentially expressed genes (DEGs) in the control and 4 hpi treatment overlapped, but most were unique to their treatment. The majority of the DEGs (34 genes) was down-regulated in the *pae9-2* mutant and enriched for responses to biotic stress (Fig. 4A).

As the *pae9-2* transcriptome was the most distinct under the control treatment, we zoomed in on these DEGs. Three gene clusters with a distinct perturbation signature across the treatments could be distinguished (Fig. 4B). Clearly, the first two clusters contained most of the constitutively down-regulated biotic stress responsive genes, which increased to the wild-type level after 4 h (cluster I) or 8 h (cluster II) of aphid infestation. The 'early' cluster I involved, for example, a wound-responsive jasmonoyl-Ile (JA-Ile) hydroxylase (the *CYTOCHROME P450 CYP94B3*) and three abscisic acid (ABA)–related genes [*NINE-CIS-EPOXYCAROTENOID DIOXYGENASE 3* (*NCED3*), *NOD26-LIKE MAJOR INTRINSIC PROTEIN 1* (*NLM1*), and *HIGHLY ABA-INDUCED PP2C GENE 1* (*HAI1*)].

The 'late' cluster II contained two genes involved in the indole phytoalexin pathway (Glawischnig, 2007): *PHYTOALEXIN DEFICIENT 3* (*PAD3*), required for camalexin biosynthesis (Zhou et al., 1999), and *INDOLE GLUCOSINOLATE O-METHYLTRANSFERASE 2* (*IGMT2*), involved in the production of 4-methoxy-indol-3-yl-methyl glucosinolate (GLS; 4MO-I3M) from 4-hydroxy-indol-3-yl-methyl GLS (4OH-I3M; Pfalz et al., 2011). Quantitative PCR (qPCR) trends confirmed down-regulation of *PAD3* and *IGMT2* in uninfested *pae9-1* and *pae9-2* mutants (Supplemental Fig. S1). Interestingly, both camalexin and indole GLSs have previously been shown to be detrimental for *M. persicae* aphids and to reduce phloem feeding (Pegadaraju et al., 2007; Kim et al., 2008; Kettles et al., 2013).

Cluster III contained mostly stably up-regulated genes with various functions. Among them was *GAST1 PROTEIN HOMOLOG 1* (*GASA1*), involved in the regulation of free radical accumulation in the cell wall (Trapalis et al., 2017), and could indicate redox stress in the cell wall. To verify if PAE9 did not affect the expression of the characterized OG-receptors *WAK1* and *WAK2* (Decreux and Messiaen, 2005; Kohorn et al., 2009), qPCR was performed. For *WAK1* no differential expression was observed, but *WAK2* showed a decreased trend in *pae9* mutants in the control (Supplemental Fig. S1). Overall, we could conclude that the *pae9-2* transcriptome was characterized by constitutively down-regulated biotic stress response genes related to JA, ABA, and indole phytoalexins.

Aphid-Induced Perturbations of the Expression of Regulatory Genes

Although the Col-0 profile of the 56 DEGs remained stable over aphid treatments (with the exception of *AT2G14878*, Supplemental Table S4), *pae9* mutants showed a significant aphid-induced up-regulation of almost 40% of the initially down-regulated genes. To see which regulatory genes could be responsible for this increase, DEGs were scanned for genes annotated as receptors, membrane channels, transcription factors, or other signaling elements. In total, 19 regulatory genes were found, of which 10 were differentially expressed between Col-0 and the *pae9-2* mutant in the 'transition phase' at 4 hpi (Table 1). Most were, however, expressed at lower levels than in the wild type and illustrated an impaired aphid-induced response in the *pae9-2* mutant. Only one kinase had a (8-fold) higher expression in the *pae9-2* mutant, *TYPE II PHOSPHATIDYLINOSITOL 4-KINASE (PI4Kγ3)*, and is involved in regulating oxidative stress (Table 1; Akhter et al., 2016).

Interestingly, *WRKY51* and *WRKY62*, both JA-pathway suppressors (Mao et al., 2007; Gao et al., 2011), were down-regulated in the *pae9-2* mutant (Table 1). qPCR confirmed reduced trends of *WRKY51* in both *pae9-1* and *pae9-2* mutants during the control and 8 hpi treatment, but not for *WRKY62* (Supplemental Fig. S1). *WRKY51* suppresses JA signaling in conditions of low availability of the JA precursor oleic acid (18:1), and down-regulation of *WRKY51* has been shown to restore JA responses (Gao et al., 2011). RNA-Seq analyses also revealed down-regulation of *WAK3* at 4 hpi,

but the function and involvement in DAMP-related processes is still unknown for this WAK (Wagner and Kohorn, 2001).

Low Constitutive Phytohormone and Camalexin Levels in *pae9* Mutants

Absolute quantification of phytohormones in the rosettes revealed that constitutive levels of JA, JA-Ile, SA, ABA, and indole-3-acetic acid (IAA) were compromised in *pae9-1* and *pae9-2* mutants (Fig. 5). Despite these consistent reductions in various growth- and stress-related phytohormones, virtually all differences between the wild-type and mutant plants disappeared within 8 h of aphid infestation. In particular, JA and JA-Ile profiles showed a strong aphid-induced up-regulation from an initial 2- to 3-fold reduction to a steep increase of JA in the first 4 h, followed by a sharp peak in the active conjugate JA-Ile between 4 and 8 h (Fig. 5). Upstream of JA, the levels of cis-(+)-12-oxo-phytodienic acid (cis-OPDA) did not show a consistent reduction.

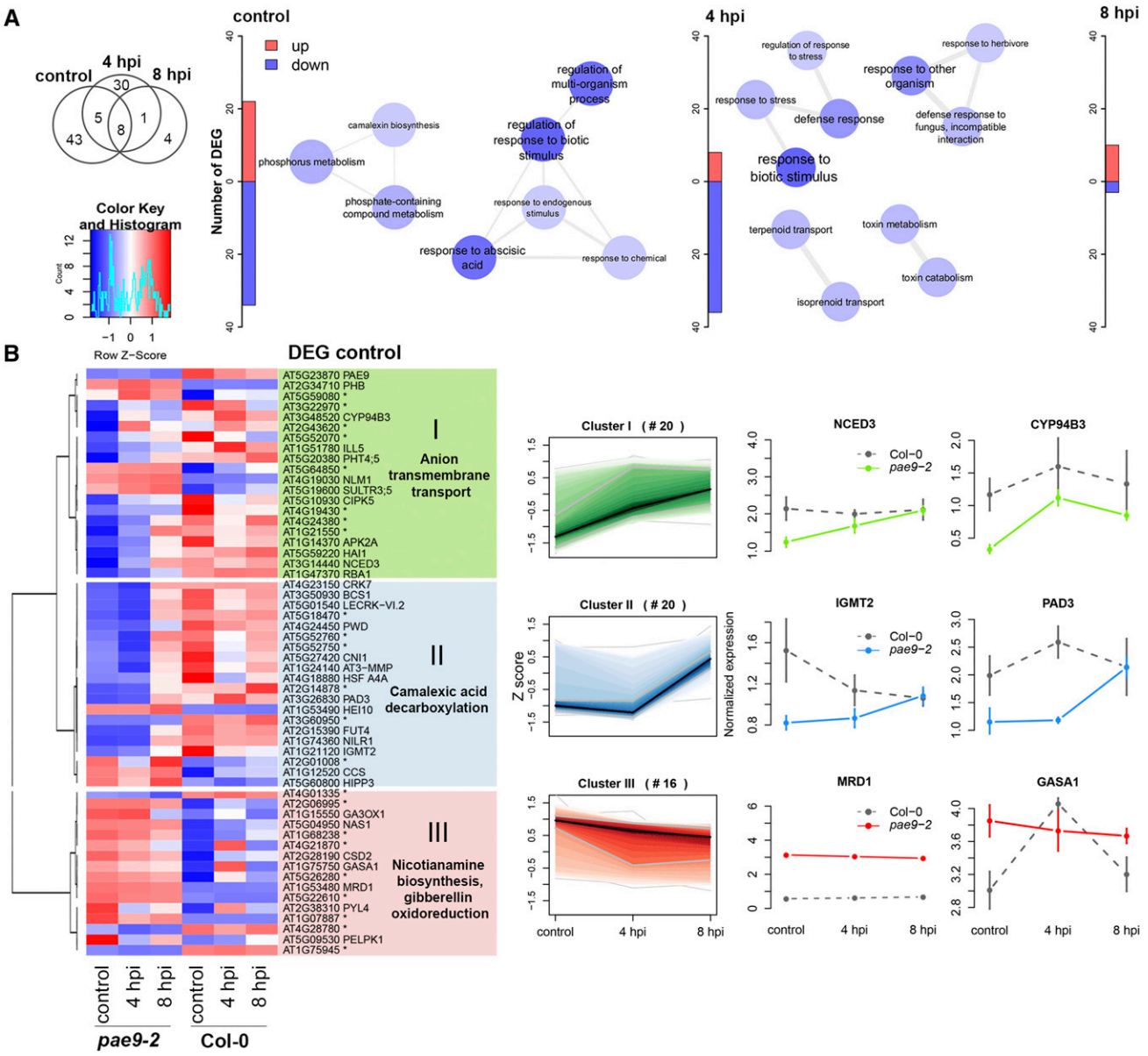

Figure 4. Transcriptome of the *pae9-2* mutant. A, The number of differentially expressed genes (DEGs) in the *pae9-2* mutant relative to Col-0, and GO enrichment of down-regulated genes. B, DEGs in the control treatment with hierarchical clustering on perturbations (Ward's minimum variance method on z-scores). Clusters are illustrated with GO enrichment, perturbation signature, and two exemplary genes (values represent mean normalized expression and bars depict SES). Genes without names are annotated with an asterisk in the heatmap.

Table 1. *Differentially expressed receptors and transcription factors and other regulating genes in the* pae9-2 *mutant (log2-fold change in comparison with the wild type)*

ns, not significant.

GeneID	Name	Control	4 hpi	8 hpi
AT1G14370	*PROTEIN KINASE 2A (APK2A)*	−1.1	ns	ns
AT1G15520	*ATP-BINDING CASSETTE G40 (ABCG40)*	ns	−2.6	ns
AT1G21240	*WALL ASSOCIATED KINASE 3 (WAK3)*	ns	−3.9	ns
AT1G47370	*RESPONSE TO THE BACTERIAL TYPE III EFFECTOR PROTEIN HOPBA1 (RBA1)*	−2.7	ns	ns
AT1G51800	*IMPAIRED OOMYCETE SUSCEPTIBILITY 1 (IOS1)*	ns	−1.9	ns
AT1G57630	*Toll-IL-Resistance (TIR) domain family protein*	ns	−2.3	ns
AT1G74360	*NEMATODE-INDUCED LRR-RLK 1 (NILR1)*	−1.3	ns	ns
AT2G38310	*PYRABACTIN RESISTANCE (PYR) 1-LIKE 4 (PYL4)*	0.7	ns	ns
AT3G04720	*PATHOGENESIS-RELATED 4 (PR4)*	ns	−1.5	ns
AT3G28930	*AVRRPT2-INDUCED GENE 2 (AIG2)*	ns	−0.8	ns
AT4G18880	*HEAT SHOCK TRANSCRIPTION FACTOR A4A (HSF A4A)*	−1.6	ns	ns
AT4G19030	*NOD26-LIKE MAJOR INTRINSIC PROTEIN 1 (NLM1)*	1.6	1.7	ns
AT4G23150	*CYS-RICH RLK (RECEPTOR-LIKE PROTEIN KINASE) 7 (CRK7)*	−2.1	−2.7	ns
AT4G39030	*ENHANCED DISEASE SUSCEPTIBILITY 5 (EDS5)*	ns	−1.4	ns
AT5G01540	*L-TYPE LECTIN RECEPTOR KINASE-VI.2 (LECRK-VI.2)*	−1.4	ns	ns
AT5G01900	*WRKY DNA-BINDING PROTEIN 62 (WRKY62)*	ns	−3.3	ns
AT5G24240	*TYPE II PHOSPHATIDYLINOSITOL 4-KINASE (PI4Kγ3)*	ns	3.2	3.3
AT5G60800	*HEAVY METAL-ASSOCIATED ISOPRENYLATED PLANT PROTEIN3 (HIPP3)*	0.9	0.9	1.1
AT5G64810	*WRKY DNA-BINDING PROTEIN 51 (WRKY51)*	ns	−2.8	ns

Relative quantification of a broader set of 97 secondary metabolites revealed that the *pae9-1* and *pae9-2* mutants segregated from the wild-type metabolome, and that the segregation was mainly due to 28 compounds (variable importance in projection [VIP] score > 1, partial least squares discriminant analysis (PLS-DA) with two components, goodness of fit: $R_1^2 = 0.74$, $R_2^2 = 0.74$, predictive ability: $Q_1^2 = 0.66$, $Q_2^2 = 0.67$, $P_{CV\text{-}ANOVA} = 0.0099$; Fig. 6, A and B; Table 2; Supplemental Table S5). The *pae9* secondary metabolome was characterized by constitutive low levels of oxylipins, SA glucoside, camalexin, and antioxidant-related metabolites, such as protocatechuic acid glucoside, syringic acid glucoside, and sinapoyl malate (Fig. 6A; Sgherri et al., 2004; Nićiforović and Abramovič, 2014). More abundant metabolites in *pae9* mutants included several flavonoids and aliphatic GLSs, such as glucoiberin and glucoraphanin (Fig. 6, A and B).

Oxylipins Remain Compromised after Aphid Infestation

The effects of PAE9 on aphid-induced perturbations in the secondary metabolome were assessed as well.

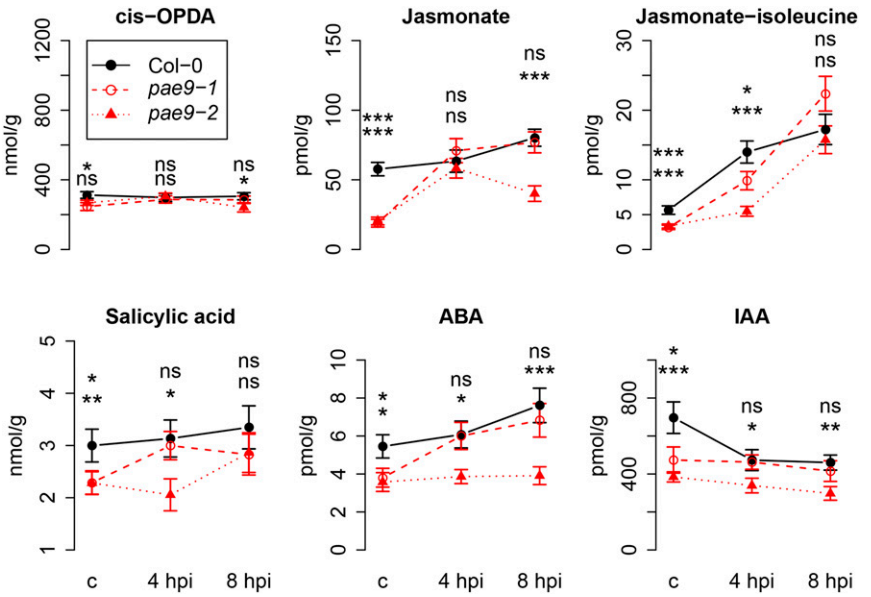

Figure 5. PAE9 effects on phytohormone content. Absolute quantification of phytohormones in uninfested plants and 4 and 8 h after *M. persicae* aphid infestation (*$P < 0.05$, **$P < 0.01$, ***$P < 0.001$, $n = 6$, linear mixed model with batch as random effect, values represent mean concentration, bars depict SES; ns, not significant).

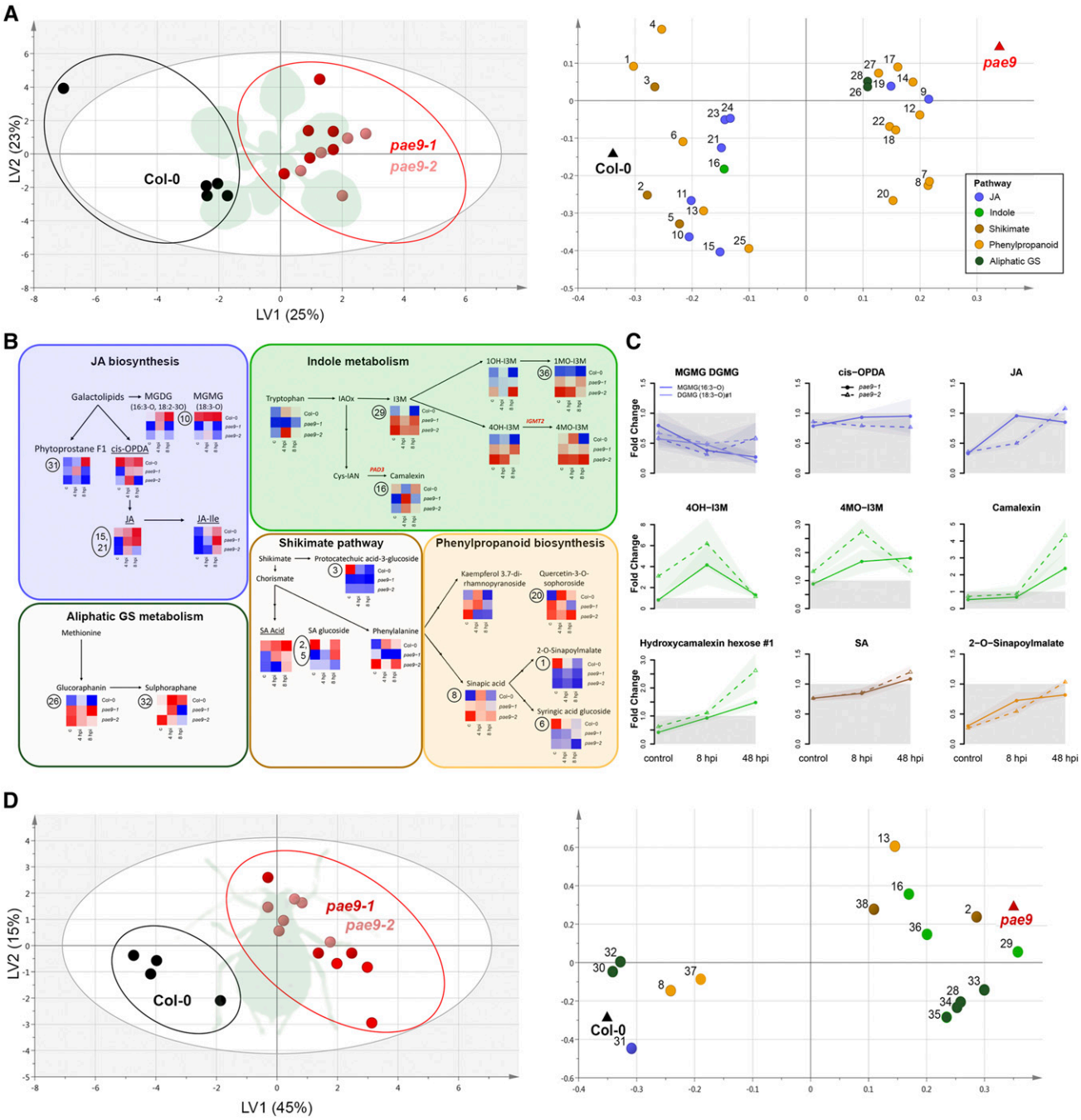

Figure 6. Secondary metabolite profile of the *pae9* mutant and wild-type rosettes and *M. persicae* aphids. A, Secondary metabolites in uninfested plants (PLS-DA based on the relative quantification of 28 secondary metabolites with VIP score > 1; Table 2; Supplemental Table S5). B, Metabolite pathways and metabolite perturbations in control, 4-hpi, and 8-hpi treatments (heatmaps: blue = low, red = high, encircled numbers refer to compounds in (A) and (D), absolute quantified phytohormone conjugates are underlined, pathways are simplified). C, Effects of 8-h and 48-h aphid infestation on *pae9-1* and *pae9-2* metabolite abundance compared with Col-0 (colored according to metabolite pathways, gray area is down-regulated, points represent mean fold change, lighter shades SE). D, Accumulation of plant secondary metabolites in aphids that had been feeding from either *pae9* mutants or Col-0 plants for 10 d (PLS-DA based on relative quantification of 15 secondary metabolites with VIP score > 1; Table 2; Supplemental Table S9). LV1, latent variable 1, LV2, latent variable 2.

Table 2. *Secondary metabolites and the plant line where they were most abundant*

Only metabolites with VIP score > 1 in control rosettes and in aphids are listed and annotated with plant line (ID, identity in loading plot (Fig. 6); *pae9* = *pae9-1* and *pae9-2*; Y = detected in phloem sap exudates). Dashes indicate VIP scores < 1.

ID	Compound	Rosettes Control	Rosettes 8 hpi	Aphids	Detected in Phloem
1	2-O-sinapoylmalate	Col-0	Col-0	—	Y
2	Salicylic acid glucoside	Col-0	—	*pae9*	Y
3	Protocatechic acid-3-glucoside	Col-0	—	—	Y
4	Sinapoylmalate-O –2-O-sinapoylmalate	Col-0	Col-0	—	N
5	Salicylic acid glucoside#1	Col-0	—	—	Y
6	Syringic acid glucoside	Col-0	—	—	Y
7	Sinapyl aldehyde	*pae9*	*pae9*	—	Y
8	Sinapic acid	*pae9*	*pae9*	Col-0	Y
9	18:1-O	*pae9*	Col-0	—	Y
10	MGMG (18:3-O)	Col-0	Col-0	—	Y
11	DGMG (18:3-O) #1	Col-0	Col-0	—	Y
12	Kaempferol-3-rhamnosie-7-rhamnosie	*pae9*	—	—	Y
13	Sinapyl 4-glucoside	Col-0	Col-0	*pae9*	Y
14	Feruloyl-glucoside	*pae9*	—	—	Y
15	(+)-Jasmonate	Col-0	Col-0	—	Y
16	Camalexin	Col-0	—	*pae9*	Y
17	Kaempferol-3-O-rham-gluco-7-O-rham	*pae9*	—	—	Y
18	Syringic acid–quinic acid	*pae9*	*pae9*	—	Y
19	11-Hydroxyjasmonates	*pae9*	—	—	Y
20	Quercetin-3-O-sophoroside	*pae9*	—	—	Y
21	(-)-Jasmonate	Col-0	—	—	Y
22	Luteolin-3′-7-di-O-glucoside	*pae9*	—	—	Y
23	MG (16:3-O)	Col-0	Col-0	—	Y
24	MGMG(16:3-O)	Col-0	Col-0	—	Y
25	Cyanidin 3-*O*-[6-*O*-(4-*O*-*β*-D-glucosyl-*p*-coumaroyl)-2-*O*-(2-*O*-sinapoyl-*β*-D-xylosyl)-*β*-D-glucosyl]-5-*O*-(6-*O*-malonyl-*β*-D-glucoside)	Col-0	—	—	N
26	Glucoraphanin	*pae9*	*pae9*	—	N
27	Kaempferol 3-O-B-glucoside-7-O-rham	*pae9*	—	—	Y
28	Glucoiberin	*pae9*	*pae9*	*pae9*	N
29	Indol-3-yl-methyl glucosinolate (I3M)	—	*pae9*	*pae9*	Y
30	4-Methylsulphinylbutyl	—	Col-0	Col-0	Y
31	Phytoprostane F1	—	Col-0	Col-0	Y
32	Sulphoraphan	—	Col-0	Col-0	Y
33	5-(Methylsulfinyl)pentyl glucosinolate	—	*pae9*	*pae9*	N
34	6-Methylsulfinylhexyl glucosinolate	—	*pae9*	*pae9*	Y
35	7-(Methylsulfinyl)heptyl glucosinolate	—	*pae9*	*pae9*	Y
36	Neoglucobrassicin (1-methoxy-3-indolylmethylglucosinolate)	—	*pae9*	*pae9*	Y
37	Kaempferol 3.7-di-O-rhamnopyranoside	—	—	Col-0	Y
38	Vanillic acid -glucoside	—	—	*pae9*	N

Some initially compromised compounds, such as camalexin, were up-regulated in *pae9* mutants after an aphid infestation period of 8 h (VIP score > 1, PLS-DA with two components, goodness of fit: $R_1^2 = 0.53$, $R_2^2 = 0.87$, predictive ability: $Q_1^2 = 0.31$, $Q_2^2 = 0.70$, $P_{CV\text{-}ANOVA} = 0.0059$; Supplemental Fig. S2; Supplemental Table S5). Higher levels of indole and aliphatic GLSs in *pae9* mutants also indicated a stronger aphid-induced response compared with wild-type plants. Oxylipins remained, however, compromised in *pae9* mutants at 8 hpi, including phytoprostane F1. Phytoprostanes are a class of cyclic oxylipins similar to jasmonates, but are formed from nonenzymatic reactions catalyzed by free radicals (Imbusch and Mueller, 2000; Mueller, 2004).

Additional analysis of the tandem mass spectrometry (MSMS) data showed that other phytoprostanes (e.g. A1, B1, D1, E1, H1, J1) accumulated more in wild-type plants than in *pae9-1* or *pae9-2* mutants at 8 hpi (Supplemental Fig. S3; Supplemental Table S6, $P = 0.012$, $P = 0.016$, $P = 0.019$, $P = 0.021$, $P = 0.04$, $P = 0.007$, $P = 0.012$, respectively, $n = 5$-6). To assess if these aphid-induced changes persisted over a longer time frame, plants were sampled and analyzed 48 hpi. No significant segregation of the wild-type and mutant profiles was found at 48 hpi (87 secondary metabolites, PLS-DA model: $P_{CV\text{-}ANOVA} > 0.05$, $n = 6$, Supplemental Table S7). Although cis-OPDA and JA were unaffected, other oxylipins remained compromised in *pae9* mutants at 48 hpi. In addition, camalexin and its hydroxylated conjugates showed a stronger induction than in Col-0 (Fig. 6C).

The Correlation Network Reveals an Oxidative Stress Cluster

With an integrative correlation network of the *pae9* transcriptome (56 DEGs) and secondary metabolome (the 28 segregating secondary metabolites of the control treatment), we explored the underlying processes that occur in *PAE9* loss-of-function plants. This network revealed five clusters of genes and metabolites ($r > 0.75$, Supplemental Fig. S4), of which one contained protocatechuic acid glucoside, known for its antioxidative and iron-chelating properties in the aglycone form (Sgherri et al., 2004), and several DEGs involved in oxidative stress. Among them were *CYS-RICH RLK (RECEPTOR-LIKE PROTEIN KINASE 7* (*CRK7*), involved in protection against apoplastic oxidative stress (Idänheimo et al., 2014); *CYTOCHROME BC1 SYNTHESIS* (*BCS1*), associated with ROS regulation at the mitochondrial outer membrane (Zhang et al., 2014); and *NEMATODE-INDUCED LRR-RLK 1* (*NILR1*), an extracellular kinase involved in nematode-induced ROS bursts (Mendy et al., 2017). As these correlations indicate the involvement of oxidation-reduction processes, we measured the total ROS content with the fluorescein DCFDA (2′,7′-Dichlorofluorescein diacetate) in wild-type and mutant rosettes. Differences could, however, not be confirmed in total ROS levels in the rosettes (Col-0 versus *pae9-1* $P = 0.32$, Col-0 versus *pae9-2* $P = 0.80$, $n = 10$, Supplemental Fig. S4).

More Camalexin and Indole GLS Content in Aphids from *pae9* Mutants

To analyze the metabolic effects of PAE9 on *M. persicae* aphids, we collected phloem sap exudates for relative quantification of secondary metabolites. In total, 83 metabolites were retrieved in the phloem sap exudates, of which 75 had been found as well in the rosettes, but no consistent differences were observed between *pae9* mutants and the wild type (PLS-DA model: $P_{CV\text{-}ANOVA} > 0.05$, Col-0 $n = 7$, *pae9-1* $n = 6$, *pae9-2* $n = 5$; Supplemental Table S8).

As the collection of phloem exudates with EDTA is vulnerable to volumetric differences and wound-induced artifacts, we also targeted the set of 97 secondary metabolites directly in aphids themselves, and compared aphids that had been reared for 10 d on *pae9-1* or *pae9-2* mutants with aphids from wild-type plants. In total, 54 secondary plant metabolites were retrieved that caused a significant segregation between mutant- and wild-type–reared aphids, mainly due to 15 compounds (VIP score > 1, PLS-DA with two components, goodness of fit: $R_1^2 = 0.77$, $R_2^2 = 0.95$, predictive ability: $Q_1^2 = 0.70$, $Q_2^2 = 0.87$, $P_{CV\text{-}ANOVA} < 0.001$; Fig. 6D; Table 2; Supplemental Table S9). Aphids from the *pae9* mutants contained lower levels of phytoprostane F1 and sulforaphane, the toxic breakdown product of the aliphatic GLS glucoraphanin (Zhang et al., 1992). They accumulated, however, more camalexin, SA-glucoside, and the indole GLSs I3M and 4MO-I3M on *pae9* mutants (Fig. 6D), suggesting that the biosynthesis of these compounds or their abundance in the phloem was more strongly induced in *pae9* mutants than in wild-type plants.

DISCUSSION

Pectin Deacetylation Effects on Plant Resistance

Since the proposition of the 'danger model' by Matzinger (1994), the awareness has grown that both self and nonself elements play a role in the induction of immune responses across biological realms. This study addresses how small changes in the cell wall can alter the secondary metabolome and defense status of a whole plant. Specifically, we characterized the downstream effects of pectin deacetylation in Arabidopsis and its impact on resistance to *M. persicae* aphids. We used *pae9* mutants as a model, as they have 15 to 20% more pectin acetyl moieties compared with wild-type Arabidopsis plants (de Souza et al., 2014). Most strikingly, PAE9-mediated pectin deacetylation up-regulated a broad range of phytohormones (JA, SA, ABA, and IAA), biotic stress-related transcripts, and antioxidant compounds. On *pae9* mutants *M. persicae* aphids established phloem feeding earlier. Later, aphid-induced responses in *pae9* mutants, involving increases in, for example, JA, JA-Ile, SA, camalexin, and GLSs (Figs. 5 and 6), overruled eventual effects on aphid fitness.

Cell Wall Penetration—no PAE9-Mediated Effects

Based on the EPG data, we can conclude that PAE9 did not affect the ability of *M. persicae* aphids to penetrate the cell wall matrix. No effects were observed on penetration difficulties in the apoplast or on the required time to the first arrival at the phloem. This is different from the effects of PMEs, which decreased the time at which *M. persicae* arrived at the phloem (Silva-Sanzana et al., 2019). We did observe that aphids spent less time on cell wall penetration on the *pae9-1* mutant, but this effect was not confirmed in the *pae9-2* mutant, and did not lead to discrepancies in feeding performance between *pae9-1* and *pae9-2* mutants. The importance of aphid effectors for the enzymatic breakdown of pectin remains yet to be investigated, and requires the testing of aphid effectors and their enzymatic activity. A relevant consideration is that aphids rely as well on mechanical force to penetrate the cell wall matrix, and might not necessarily need enzymatic support. Force is the product of mass and acceleration. Unlike microorganisms, aphids can use both their body weight (about 500 μg for 1 adult *M. persicae* aphid [Cao et al., 2016]) and musculature at the stylet base to push their mandibles into the host. The aphid stylet base has a diameter of 1.5 to 3 μm at the upper segments, which tapers to about

0.04 μm at the stylet tip. Pressure applied to the relatively large base will transform to a greater force per unit area at the stylet tip (Dixon, 1973). Figure 2 gives us an idea of the acceleration of the penetration. This *M. persicae* aphid penetrated its stylet through at least 26 μm of cell wall at an overall speed of 2.0 μm per minute (excluding the time spent on intracellular activities and movements in the direction of the z axis). The actual penetration speed is, however, not constant, as aphids penetrate in short bouts in between intracellular activities. The aphid in Fig. 2, for example, performed 27 distinct cell wall penetrations with a duration of 25 to 45 s each. Every single penetration requires acceleration of the stylet and thus the application of mechanical force. The additional requirement of enzymatic breakdown of cell wall components will, nevertheless, depend on aphid and plant species. Particularly for perennial host plants with a high lignin content or thick carbohydrate matrix, aphids might require more enzymatic support. This will likely be reflected in the diversity of secretory carbohydrate-active enzymes across genera of Hemipterans.

Delay in Phloem Feeding Is Associated with Camalexin

On *pae9* mutants, aphids established phloem feeding earlier than on wild-type plants (Fig. 3A). EPG recordings illustrated that aphids were less prone to interrupt feeding and engaged less in 'nonprobing' activities in the first 8 h. 'Nonprobing,' that is, not making contact with the host via their stylets, is considered to happen less frequently and shorter when aphids accept their host plant and engage in sustained phloem feeding (Tjallingii, 1994). One of the key questions is this: What factor(s) caused the PAE9-mediated reduction in phloem feeding (Fig. 3A)? As this phenotype manifested in the first hours of plant-aphid contact, a constitutive mechanism is to be expected. The involvement of indole glucosinolates, which are known to have antifeedant effects on *M. persicae* (Kim et al., 2008), was postulated due to the down-regulation of *IGMT2*, but could not be confirmed by the accumulation of 4OH-I3M and 4MO-I3M in uninfested plants. Instead, both transcriptomic and metabolomic data showed that camalexin was compromised, as *pae9* mutants had a down-regulated transcription of the camalexin biosynthesis gene *PAD3* (Fig. 4B; Supplemental Fig. S1) and contained lower levels of camalexin and its hydroxylated conjugates than Col-0 when uninfested (Fig. 6A; Table 2). Our observation of earlier establishment of phloem feeding on the camalexin-compromised *pae9* mutants is consistent with the previously reported increase in *M. persicae* phloem feeding on *pad4* mutants with impaired camalexin production (Pegadaraju et al., 2007). That we did not observe higher *M. persicae* reproductive rates on plants with less camalexin, as shown by Kettles et al. (2013), can be explained by the induction of camalexin upon aphid infestation. Our metabolomic data showed that *pae9* mutants had a stronger induction of camalexin than wild-type plants (Fig. 6C) and that aphids that had been living on *pae9* mutants accumulated more camalexin (Fig. 6D). From this, even a lower aphid fitness on *pae9* mutants would have been expected. Other factors, such as the increased accumulation of phytoprostane F1 and sulphoraphan in aphids from wild-type plants (Table 2; Fig. 6D), might have had a detrimental impact on their fitness as well.

Rapid Up-Regulation of Defenses in Low JA Condition

Even though PAE9 loss of function resulted in low constitutive levels of JA and the indole phytoalexin pathway, PAE9 was not required for aphid-induced plant responses. Impressively, plants without PAE9 increased their initially compromised transcriptome and JA, GLS, and camalexin profiles almost to wild-type levels within 8 h of aphid infestation. This rapid increase in defense-related transcripts and secondary metabolites can explain the reduction in *pae9* plant biomass after infestation (which was not observed in plants without aphids; Fig. 3B), as strong defense responses are expected to come at a cost (Neilson et al., 2013). Nevertheless, it is surprising that GLSs accumulated so strongly in *pae9* mutants with reduced JA availability. If JA levels are too low for proper induction of GLS biosynthesis, plants can adjust the regulatory switches downstream in the JA pathway to compensate. A good example is the *suppressor of SA insensitivity2* (*ssi2*) mutant with compromised oleic acid (18:1), which restores its JA responsiveness when *WRKY50* or *WRKY51* are knocked out (Gao et al., 2011). These WRKYs are suppressors of JA-mediated signaling and act in conditions with low availability of JA precursors. Interestingly, we observed down-regulation of *WRKY51* in the *pae9-2* mutant and similar trends in the *pae9-1* mutant (Table 1; Supplemental Fig. S1). By releasing this suppressor, JA-responsive processes, such as GLS biosynthesis, can increase irrespective of the compromised availability of oxylipins in these mutants.

PAE9's Mode of Action: DAMPs and ROS

Even though this study focused on the effects of PAE9 on the defense status of the plant, our data contain some relevant information about PAE9's mode of action. Interestingly, the whole genome transcriptome did not include differential expression of the DAMP-related genes *WAK1* and *WAK2* (Decreux and Messiaen, 2005; Kohorn et al., 2009). Validation with qPCR revealed, nevertheless, a slight reduction in *WAK2* in uninfested *pae9* mutants (Supplemental Fig. S1). *WAK2* is an OG-receptor, which is involved in the accumulation of ROS (Kohorn et al., 2012). OG-mediated signaling via WAK2 or changes in redox status due to PAE9-mediated pectin cross-linking (Fig. 1) are possibly responsible for the observed oxidative stress signature in the *pae9* transcriptome and metabolome. Several oxidative stress-related genes

were differentially expressed, such as the ROS signaling kinase *CRK7* (Idänheimo et al., 2014), the hydrogen peroxide sensitive aquaporin *NLM1* (Sadhukhan et al., 2017), the superoxide dismutase *CSD2* (Podgórska et al., 2017), and the superoxide dismutase chaperone *AtCCS* (Abdel-Ghany et al., 2005). Also, many antioxidant metabolites were identified in the PLS-DA models, such as protocatechuic acid glucoside, sinapoylmalate, and phytoprostanes (Landry et al., 1995; Mueller, 2004; Sgherri et al., 2004; Williams et al., 2012). In addition, the main groups of compromised metabolites in uninfested plants, i.e., oxylipins and camalexin, can also be formed by nonenzymatic oxidation reactions (Imbusch and Mueller, 2000; Böttcher et al., 2009). Quantification of ROS with DCFDA, however, did not confirm an effect of PAE9 on the total ROS pool in whole leaves (Supplemental Fig. S4). Apoplastic differences in specific ROS types, such as hydrogen peroxide or hydroxyl radicals, in the apoplast might, nevertheless, be interesting for further investigation. In contrast with peroxidase-dependent 'ROS bursts' upon pathogen infection (Bindschedler et al., 2006), constitutive ROS homeostasis in the apoplast is a delicate balance in oxidation-reduction processes that controls cross-linking of cell wall polymers and cell expansion (Pelloux et al., 2007; Kärkönen and Kuchitsu, 2015; Schmidt et al., 2016). Depending on the ROS type, cell wall polymers become cross-linked (via hydrogen peroxide) or loosened (via hydroxyl radicals). ROS accumulate easily in the low antioxidant environment of the apoplast and can rapidly induce Ca^{2+} fluxes into the cell that trigger (a)biotic stress responses (Podgórska et al., 2017; Waszczak et al., 2018). On top of that, pectin modifications influence the OG abundance and their binding capacity to WAKs (Decreux and Messiaen, 2005; Pogorelko et al., 2013a; Bethke et al., 2014), which regulate intracellular ROS accumulation. We expect, therefore, that defects in pectin deacetylation, as in the condition of *pae9* mutants, will affect the ROS status of the plant.

Aphid Induction of Phytoprostanes

Here, we describe that *M. persicae* aphids induce a wide range of phytoprostanes in Arabidopsis. An up-regulation of up to 3-fold was observed within 8 h of infestation, depending on the type of phytoprostane (Supplemental Fig. S3). All nine phytoprostanes (A1, B1, D1, E1, F1, G1, H1, J1, and an unknown conjugate) were identified in both rosette material and phloem sap exudates, implying that these compounds are likely to be ingested by phloem-feeding insects. We could, however, only retrieve phytoprostane F1 in aphids (Fig. 6D; Table 2). As some phytoprostanes up-regulate mitogen-activated protein kinases and camalexin biosynthesis (Thoma et al., 2003), further investigation of their role in aphid resistance would be of interest. Relative quantification showed that the aphid-induced up-regulation of phytoprostanes was absent in *pae9* mutants. Phytoprostanes are formed via free-radical-catalyzed lipid peroxidation (Imbusch and Mueller, 2000). Whether the compromised phytoprostane levels in *pae9* mutants can be attributed to an altered redox state or simply to a reduced pool of oxylipins remains to be investigated. The decline in jasmonate, phytoprostane, and related oxylipin levels nevertheless illustrates that PAE9-mediated pectin deacetylation affects the oxylipin pathway.

An Applied Perspective for Pectin Deesterification

In this study, we showed that PAE9-mediated pectin deacetylation increased constitutive levels of JA and SA and biotic stress-related transcripts. But how relevant is this for pest and disease management? From our lab study it is clear that the effects of 15% to 20% more pectin deacetylation in Arabidopsis are still marginal for *M. persicae* aphids. Taken into consideration that these experiments involved no-choice assays, where the aphids were either glued to a 1- to 2-cm wire or isolated on a single plant, field situations might reveal larger impacts. Constitutive resistance usually has negative impacts on host plant acceptance in more natural situations (Schoonhoven et al., 2005). In greenhouses and fields, aphids may give up their attempts to feed and choose to leave crop fields. Whether other PAEs have similar effects on the defense status of plants remains to be investigated. Furthermore, the resistance effect could be enhanced by combining several cell wall traits. Silva-Sanzana et al. (2019) showed that PME activity resulted in increased phloem feeding by *M. persicae* aphids. It is interesting that both PME and PAE activity affect the phloem feeding stage, which suggest that both pectin modifications induce changes in the constitution of the phloem sap. Potentially, reduced PME and increased PAE activity combined would further enhance plant resistance to *M. persicae* aphids. Together with insights in downstream plant physiological responses on, for example, fruit set and resistance to other biotic stresses, pectin deesterification could be exploited as an integrative tool in sustainable pest and disease management.

MATERIALS AND METHODS

Plants and Insects

The Arabidopsis (*Arabidopsis thaliana*). Col-0 accession (CS60000) and the T-DNA lines SALK_046973 (*pae9-1*) and GABI_803G08 (*pae9-2*), both in the Col-0 background, were obtained from the European Arabidopsis Stock Centre. Homozygous T-DNA plants were selected by PCR (primers listed in Supplemental Table S10) and harvested for seeds for subsequent experiments. Absence of expression of *PAE9* was validated by qPCR. Arabidopsis seeds were cold stratified for 72 h at 4°C before they were sown into pots (6-cm diameter) with a 4:1 mixture of potting soil (Yrkes plantjord, den Gröna linjen) and vermiculite (Agra-vermiculite; 4:1). Plants were grown in a climate cabinet at 23 ± 0.5°C, with a light intensity of 180 μmol m^{-2} s^{-1} (Philips Silhouette High Output F54T5/841 HO), 50% to 70% relative humidity, and an 8 h:16 h light (L):dark (D) photoperiod for aphid reproduction, transcriptome, and metabolome experiments, and a 12 h:12 h light (L):dark (D) photoperiod for EPG experiments. Green peach aphids, *Myzus persicae* (Sulzer), were reared on radish [*Raphanus sativus* (L.)] at 21 ± 0.5°C, 50% to 70% relative humidity, and

an 8 h:16 h L:D photoperiod. For all experiments that involved aphids, only wingless aphids were used, and a water bath with detergent surrounded infested plants to prevent escape to other hosts.

EPG Recording, Cryofixation, and Aphid Population Assay

EPG recording of adult *M. persicae* aphids was performed on 5-week-old plants. Direct currents were used according to the methodology of ten Broeke et al. (2013). Aphids were radish-reared and, to adapt to Arabidopsis, aphids were transferred to Col-0 Arabidopsis plants 1 d before the experiments to habituate aphids to Arabidopsis as a host. Each biological replicate consisted of one unique plant and aphid. Aphids were used as an electrode by gently attaching an 18 μm diameter gold wire of 1.5 cm to the dorsum with silver glue. Electrical signals associated with stylet activities were recorded and annotated with EPG Stylet+ software (Tjallingii, 1988; http://www.epgsystems.eu) and further processed in R (R Core Team, 2017). Summary values of the 8-h recording were analyzed with Mann Whitney *U* tests (Supplemental Table S1). Patterns over time were assessed by calculating the time spent on each behavior per time bin of 1 h. Data were analyzed with a linear mixed model with plant line and time and the interaction between plant line and time as fixed factors using the R package nlme (Supplemental Table S2; Pinheiro and Bates, 2018). Cryofixation of aphids was performed according to the methodology of Walker and Medina-Ortega (Walker and Medina-Ortega, 2012). In brief, aphids were attached to the EPG on the abaxial side of a leaf of an intact Col-0 plant and cryofixed during phloem feeding by pouring liquid nitrogen-chilled ethanol on the adaxial side of the leaf. Leaves with stylet still inserted were stored in ethanol at −80°C until further processing. After being gradually brought to room temperature, samples were casted in 5% (w/v) agar and sectioned with a Leica VT1000S vibratome. Sections (120 μm thick) were stained with 0.05% (w/v) toluidine blue (in water) for 20 to 30 s. Images were taken with an AxioCam HRc digital camera (Zeiss) mounted on an Axioplan 2 light microscope (Zeiss). For the aphid population assay, 3-week-old Arabidopsis plants were infested with one founder aphid. To minimize bias in the reproductive output, we used neonate aphids (between 1 and 24 h old). Infested plants were placed in a climate cabinet at 23 ± 0.5°C, 50 to 70% relative humidity, an 8 h:16 h L:D photoperiod, and 180 μmol m^{-2} s^{-1} light intensity (Philips Silhouette High Output F54T5/841 HO). From d 6 onward, occurrence of the first offspring was checked twice per day using 3× magnification glasses. The total number of aphids per plant was counted 14 d after infestation. Aphid numbers were analyzed with a mixed model with the plant line as a fixed factor and plant fresh weight as random effect. Plant fresh weight was analyzed with a one-way ANOVA.

Collection of Rosette Material for RNA Sequencing and Metabolomics

Two to three Arabidopsis plants were grown per 6 × 6 cm pot. At the age of 3 weeks, the pots were randomly assigned to one of the following treatments: no aphids (control treatment), 4-h aphid infestation, or 8-h aphid infestation. For the aphid treatments, each plant was infested with 20 wingless aphids, both nymphs and adults. Sampling was done in two separate batches in a complete block design. The 48-hpi treatment was sampled in a separate batch from the other treatments. Other samples were harvested in two batches with treatments equally represented per batch. To minimize batch handling differences and individual effects, harvest was limited in time (12–4 PM) and rosettes within a pot were pooled into one sample. Leaves were gently wiped with a soft brush to remove aphids. Plants without aphids were brushed similarly as a control treatment. Samples were flash-frozen in liquid nitrogen, homogenized, and stored at −80°C until further processing.

Collection of Phloem Exudates and Aphid Samples for Metabolomics

Phloem exudates were collected according to adapted methodologies of Stolpe et al. (2017) and Tetyuk et al. (2013). For each sample, 15 fully grown leaves of three 6-week-old Arabidopsis plants (without aphids) were cut at the base of the petiole with a razor blade and immediately immerged in a petri dish with 8 mM EDTA (pH 8). Once all 15 leaves were cut, they were stacked on top of each other and freshly cut again at the base of the petiole. To wash the cutting surface on the petioles the stacked leaves were gently transferred to an Eppendorf tube with 1-mL 8 mM EDTA (pH 8) for 5 min with petioles submerged and leaf blades sticking out from the open tube. Subsequently, the stacked leaves were transferred to a fresh Eppendorf tube with 1-mL 8 mM EDTA (pH 8) for exudation. To prevent dehydration, the tubes with leaves were placed in a dark container with wet towels and vents at 21°C. After 6 h, the exudates were flash-frozen in liquid nitrogen and lyophilized for 24 h. The leaves were dried at 65°C for 72 h. Metabolomic measurements were corrected for leaf dry weight. Aphids were collected for metabolomics analyses after 10 d of infestation on either 5-week-old Col-0, *pae9-1*, or *pae9-2* plants. One biological sample consisted of 10 to 20 mg of aphids (fresh weight) collected from 1 to 2 unique plants. After collection, aphids were flash-frozen in liquid nitrogen and lyophilized for 24 h.

RNA-Seq and qPCR

RNA was isolated from rosette material with a PureLink RNA Mini kit, and treated with Ambion TURBO DNA-free according to the manufacturer's instructions. With an Agilent 2100 Bioanalyzer, samples were confirmed to have an RNA Integrity Number > 8. RNA contamination was checked with a NanoDrop ND-1000 spectrophotometer, and when necessary, RNA was cleaned with GeneJet RNA Cleanup and Concentration Micro Kit in order to have OD 260/280 ≥ 2 and OD 260/230 ≥ 1.7. RNA was quantified with an Invitrogen Qubit fluorometer. Libraries were prepared with an Illumina TruSeq Stranded mRNA kit with Poly-A selection and sequenced for 2× 126 bp paired end with Illumina HiSeq 2500 High Output V4 in 2 lanes, multiplexed with 27 samples per lane. For qPCR of *PAE9*, RNA isolation and DNase treatment were performed according to the methods above. RNA integrity was assessed with electrophoresis in a 1% (w/v) agarose gel stained with GelRed Nucleic Acid Gel Stain. DNA-free RNA was converted into cDNA using the Bio-Rad iScript cDNA Synthesis Kit. Quantitative PCR was performed on a Roche LightCycler 480 II using LightCycler 480 SYBR Green I Master mix, and the primers described in Supplemental Table S10. For qPCR of other genes, RNA was isolated with the Bioline ISOLATE II RNA Plant Kit, treated with Promega RQ1 RNase-Free DNase, converted into cDNA with the SensiFAST cDNA Synthesis Kit, and processed on a Biorad CFX96 Touch Real-Time PCR detection system with the SensiFAST SYBR No-ROX Kit. Two technical replicates of each sample were taken into account and gene expression was normalized with the weighted average of two reference genes.

RNA-Seq Data Processing and Analysis

Data preprocessing was performed according to the Epigenesys guidelines(http://www.epigenesys.eu/en/protocols/bio-informatics/1283-guidelines-for-rna-seq-data-analysis). In brief, raw sequence quality was assessed with FastQC v0.11.4 (http://www.bioinformatics.babraham.ac.uk/projects/fastqc/) and summarized with MultiQC v1.3 (http://multiqc.info/). Residual rRNA contamination was determined and removed using SortMeRNA v2.1, settings *–log–paired_in–fastx–sam–num_alignments 1* (Kopylova et al., 2012) using the rRNA sequences provided with SortMeRNA (rfam-5s-database-id98.fasta, rfam-5.8s-database-id98.fasta, silva-arc-16s-database-id95.fasta, silva-bac-16s-database-id85.fasta, silva-euk-18s-database-id95.fasta, silva-arc-23s-database-id98.fasta, silva-bac-23s-database-id98.fasta and silva-euk-28s-database-id98.fasta). Adapters were removed and data were trimmed for quality with Trimmomatic v0.36, settings *TruSeq3-PE-2.fa:2:30:10 SLIDINGWINDOW:5:20 MINLEN:50* (Bolger et al., 2014). A second FastQC quality control was performed to ensure that no technical artifacts had been introduced. Read counts were obtained with kallisto v0.43.0 settings *quant -b 100–pseudobam -t 1–rf-stranded* (Bray et al., 2016) using the ARAPORT11 cDNA sequences as a reference (Cheng et al., 2017). Abundance values where imported into R v3.4.3 (R-Core-Team, 2017) using Bioconductor v3.6 (Gentleman et al., 2004) tximport package (Soneson et al., 2015). Read counts were normalized using a variance stabilizing transformation as implemented in DESeq2 v1.14.1 (Love et al., 2014) using batch + treatment * plant line as the design. Custom-made R scripts were written for downstream analyses. Plant lines were compared within treatment, and only DEGs with an adjusted P value < 0.01 and a log2 fold change ≥ 0.5 were considered (Schurch et al., 2016). DEGs in the control treatment were clustered based on the z-scores of normalized expression in the *pae9-2* mutant with Ward's method and Pearson correlation tests. Heatmaps were constructed with the R package gplots v3.0.1 (https://www.rdocumentation.org/packages/gplots/versions/3.0.1). Pertubations per gene cluster were visualized with the LSD R package (Schwalb et al., 2018). DEGs were tested for overrepresentation of biological processes against a reference set including all transcripts in the complete data set with at least one count, using the application BiNGO in Cytoscape (Maere et al., 2005; Cline et al., 2007). Redundant gene ontology (GO) terms were removed and GO networks were inferred with REViGO (Supek et al.,

2011). The custom R scripts used for the analyses are available from our GitHub repository: https://github.com/UPSCb/UPSCb/blob/master/manuscripts/Kloth2018. The RNA-Seq data are available from the European Nucleotide Archive (ENA, https://ebi.ac.uk/ena) under the accession number PRJEB27944.

Phytohormone Quantification

Endogenous levels of jasmonates (JA; JA-Ile; cis-OPDA), IAA, ABA, and SA were determined in 20 mg of rosette material according to the method described by Floková et al. (2014). All experiments were repeated as six biological replicates. The phytohormones were extracted using an aqueous solution of methanol (10% [v/v] methanol:water). A cocktail of table isotope-labeled standards was added as follows: 5 pmol of [$^{13}C_6$]IAA; 10 pmol of [$^{2}H_6$]JA, [$^{2}H_2$]JA-Ile, and [$^{2}H_6$]ABA; 20 pmol of [$^{2}H_4$]SA and [$^{2}H_5$]OPDA (all from Olchemim) per sample for metabolite quantification. The extracts were purified using Oasis HLB columns (30 mg/1 mL, Waters), and targeted analytes were eluted using 80% (v/v) methanol. Eluent containing neutral and acidic compounds was gently evaporated to dryness under a stream of nitrogen. Separation was performed on an Acquity UPLC System (Waters) equipped with an Acquity UPLC BEH C18 column (100 × 2.1 mm, 1.7 μm; Waters), and the effluent was introduced into the electrospray ion source of a triple quadrupole mass spectrometer Xevo TQ-S MS (Waters). Data were corrected for sample weight and analyzed per phytohormone and treatment (control, 4 hpi or 8 hpi) with a linear mixed model with plant line as the fixed effect and batch (as described in the above paragraph) as random effect using the R packages lme4 and stargazer (Bates et al., 2015; Hlavac, 2018).

Metabolomics

Other metabolites were extracted from 20-mg leaves and 100-mg freeze dried aphids of each treatment in 1 mL of extraction buffer (methanol, chloroform, and water 20:60:20, v/v) including internal standards (Gullberg et al., 2004). Then, 100 μL of each sample was dried, dissolved in 20 μL methanol, and then diluted with 20 μL water. For phloem exudates, 1-mL per sample was suspended in 300 μL 50% (v/v) methanol:water, then applied on a SPE-C18 column, where polar compounds (like sugar and EDTA) were washed out with 1% (v/v) acetic acid and the resulting metabolites were recovered in 100% methanol. The resulting fraction was dried in a speedvac, and then dissolved in 20 μL methanol and diluted with 20 μL water. Samples from leaves, phloem exudates, and aphids were analyzed according to Adolfsson et al. (2017), and the metabolites were detected with an Agilent 6540 Q-TOF mass spectrometer equipped with an electrospray ion source operating in positive ion mode. The MSMS spectra were obtained in the same conditions, with the collision energy from 10 to 40 V. The generated mass files were processed using Profinder B.07.00 (Agilent Technologies) using mass feature extraction and find-by-ion algorithms for peak detection. The generated data were normalized against the internal standard and weight of each sample. The metabolite annotation was performed by comparison of MSMS spectra generated during the analysis with the "in house" Arabidopsis database or manual spectra interpretation of unknown metabolites. Partial Least Squares Discriminant Analysis (PLS-DA) was performed with the software SIMCA 15. PLS-DA models were inferred from complete data sets. If these models showed a significant segregation between the wild type and mutants ($P < 0.05$), a subsequent PLS-DA model was built containing only the metabolites with a VIP score higher than 1. Integrative correlation networks were built with Cytoscape (version 3.4.0) using the app ExpressionCorrelation (http://www.baderlab.org/Software/ExpressionCorrelation, absolute edge cutoff ≥ 0.75, organic graphical yFile layout). Fold changes were calculated by dividing the relative metabolite abundance of each mutant sample by the mean of the Col-0 samples within each treatment.

ROS Measurements

Total ROS content was measured with DCFDA (Sigma-Aldrich https://www.sigmaaldrich.com/catalog/product/sigma/d6883?lang=en&region=NL) according to the methodology of Jambunathan (2010). Rosettes were collected from 4-week-old plants and instantly frozen in liquid nitrogen. A 10× dilution was made from the supernatant of centrifuged samples of 10 mM Tris-HCl buffer (pH 7.2) and 50 mg homogenized rosette material. To each 200 μL sample, 2 μL 1 mM DCFDA was added, vortexed, and incubated in the dark at room temperature for 10 min. Relative fluorescence intensity was measured with a DS-11 DeNovix fluorometer (www.denovix.com), with an excitation filter of 490–558 nm and an emission filter of 514–567 nm. For each sample, the average of two technical replicates was corrected for total protein content, measured with a Bradford assay. For each undiluted 200 μL sample, 10 μL of Bradford reagent (1:4 Bradford reagent:distilled water) was added (Bio-Rad Bradford reagent www.bio-rad.com/featured/en/bradford-assay.html) and incubated for 10 min. Absorbance was measured with a BMG Labtech Optima microplate reader (www.bmglabtech.com) at 620 nm excitation. Three technical replicates were performed, and total protein content was calculated using a standard curve with 6 measuring points.

Accession Numbers

Sequence data from this article can be found in the Arabidopsis Information Resource or GenBank/EMBL data libraries under the accession numbers mentioned in Supplemental Table S4.

SUPPLEMENTAL DATA

The following supplemental materials are available.

Supplemental Table S1. EPG table with summary statistics.

Supplemental Table S2. EPG table with time bin analysis.

Supplemental Table S3. RNA-Seq sample overview.

Supplemental Table S4. Differentially expressed genes.

Supplemental Table S5. Secondary metabolites of rosettes (control and 8 hpi).

Supplemental Table S6. Phytoprostanes of rosettes.

Supplemental Table S7. Secondary metabolites of rosettes (48 hpi).

Supplemental Table S8. Secondary metabolites of phloem exudates.

Supplemental Table S9. Secondary metabolites of aphids.

Supplemental Table S10. Primers.

Supplemental Figure S1. qPCR results.

Supplemental Figure S2. PLS-DA of secondary metabolites 8 hpi.

Supplemental Figure S3. Phytoprostane perturbations.

Supplemental Figure S4. Integrative correlation network and ROS measurements.

ACKNOWLEDGMENTS

We acknowledge the Swedish Metabolomics Centre for technical support and the Science for Life Laboratory, the National Genomics Infrastructure funded by the Swedish Research Council, and Uppsala Multidisciplinary Center for Advanced Computational Science for assistance with massively parallel sequencing and access to the UPPMAX computational infrastructure. We thank Ewa Mellerowicz, Gregory Walker, Karin Ljung, and two anonymous reviewers for valuable advice and comments.

Received May 28, 2019; accepted September 9, 2019; published September 24, 2019.

LITERATURE CITED

Abdel-Ghany SE, Burkhead JL, Gogolin KA, Andrés-Colás N, Bodecker JR, Puig S, Peñarrubia L, Pilon M (2005) AtCCS is a functional homolog of the yeast copper chaperone Ccs1/Lys7. FEBS Lett **579:** 2307–2312

Adolfsson L, Nziengui H, Abreu IN, Šimura J, Beebo A, Herdean A, Aboalizadeh J, Široká J, Moritz T, Novák O, et al (2017) Enhanced secondary- and hormone metabolism in leaves of arbuscular mycorrhizal *Medicago truncatula*. Plant Physiol **175:** 392–411

Akhter S, Uddin MN, Jeong IS, Kim DW, Liu XM, Bahk JD (2016) Role of Arabidopsis AtPI4Kγ3, a type II phosphoinositide 4-kinase, in abiotic stress responses and floral transition. Plant Biotechnol J **14:** 215–230

Albersheim P, Jones TM, English PD (1969) Biochemistry of the cell wall in relation to infective processes. Annu Rev Phytopathol **7:** 171–194

Aldington S, McDougall GJ, Fry SC (1991) Structure-activity relationships of biologically active oligosaccharides. Plant Cell Environ **14:** 625–636

Bacete L, Mélida H, Miedes E, Molina A (2018) Plant cell wall-mediated immunity: Cell wall changes trigger disease resistance responses. Plant J **93:** 614–636

Bates D, Mächler M, Bolker B, Walker S (2015) Fitting linear mixed-effects models using lme4. Journal of Statistical Software **67:** 48

Bethke G, Grundman RE, Sreekanta S, Truman W, Katagiri F, Glazebrook J (2014) Arabidopsis PECTIN METHYLESTERASEs contribute to immunity against *Pseudomonas syringae*. Plant Physiol **164:** 1093–1107

Bethke G, Thao A, Xiong G, Li B, Soltis NE, Hatsugai N, Hillmer RA, Katagiri F, Kliebenstein DJ, Pauly M, Glazebrook J (2016) Pectin biosynthesis is critical for cell wall integrity and immunity in *Arabidopsis thaliana*. Plant Cell **28:** 537–556

Bi R, Berglund J, Vilaplana F, McKee LS, Henriksson G (2016) The degree of acetylation affects the microbial degradability of mannans. Polym Degrad Stabil **133:** 36–46

Bidhendi AJ, Geitmann A (2016) Relating the mechanics of the primary plant cell wall to morphogenesis. J Exp Bot **67:** 449–461

Biely P, MacKenzie CR, Puls J, Schneider H (1986) Cooperativity of esterases and xylanases in the enzymatic degradation of acetyl xylan. Nat Biotechnol **4:** 731–733

Bindschedler LV, Dewdney J, Blee KA, Stone JM, Asai T, Plotnikov J, Denoux C, Hayes T, Gerrish C, Davies DR, et al (2006) Peroxidase-dependent apoplastic oxidative burst in Arabidopsis required for pathogen resistance. Plant J **47:** 851–863

Blackman RL, Eastop VF (2006) Aphids on the World's Herbaceous Plants and Schrubs, Vol 2 The Aphids. John Wiley & Sons, Ltd. & Natural History Museum, London

Bolger AM, Lohse M, Usadel B (2014) Trimmomatic: A flexible trimmer for Illumina sequence data. Bioinformatics **30:** 2114–2120

Böttcher C, Westphal L, Schmotz C, Prade E, Scheel D, Glawischnig E (2009) The multifunctional enzyme CYP71B15 (PHYTOALEXIN DEFICIENT3) converts cysteine-indole-3-acetonitrile to camalexin in the indole-3-acetonitrile metabolic network of *Arabidopsis thaliana*. Plant Cell **21:** 1830–1845

Bray NL, Pimentel H, Melsted P, Pachter L (2016) Near-optimal probabilistic RNA-seq quantification. Nat Biotechnol **34:** 525–527

Brutus A, Sicilia F, Macone A, Cervone F, De Lorenzo G (2010) A domain swap approach reveals a role of the plant wall-associated kinase 1 (WAK1) as a receptor of oligogalacturonides. Proc Natl Acad Sci USA **107:** 9452–9457

Cabrera JC, Boland A, Messiaen J, Cambier P, Van Cutsem P (2008) Egg box conformation of oligogalacturonides: The time-dependent stabilization of the elicitor-active conformation increases its biological activity. Glycobiology **18:** 473–482

Caffall KH, Mohnen D (2009) The structure, function, and biosynthesis of plant cell wall pectic polysaccharides. Carbohydr Res **344:** 1879–1900

Cao H-H, Liu H-R, Zhang Z-F, Liu T-X (2016) The green peach aphid *Myzus persicae* perform better on pre-infested Chinese cabbage *Brassica pekinensis* by enhancing host plant nutritional quality. Sci Rep **6:** 21954

Cheng CY, Krishnakumar V, Chan AP, Thibaud-Nissen F, Schobel S, Town CD (2017) Araport11: A complete reannotation of the *Arabidopsis thaliana* reference genome. Plant J **89:** 789–804

Cherqui A, Tjallingii WF (2000) Salivary proteins of aphids, a pilot study on identification, separation and immunolocalisation. J Insect Physiol **46:** 1177–1186

Cline MS, Smoot M, Cerami E, Kuchinsky A, Landys N, Workman C, Christmas R, Avila-Campilo I, Creech M, Gross B, et al (2007) Integration of biological networks and gene expression data using Cytoscape. **2:** 2366–2382

Cosgrove DJ (2005) Growth of the plant cell wall. Nat Rev Mol Cell Biol **6:** 850–861

Cosgrove DJ (2015) Plant expansins: Diversity and interactions with plant cell walls. Curr Opin Plant Biol **25:** 162–172

Creelman RA, Mullet JE (1997) Oligosaccharins, brassinolides, and jasmonates: Nontraditional regulators of plant growth, development, and gene expression. Plant Cell **9:** 1211–1223

Davis KR, Darvill AG, Albersheim P (1986) Several biotic and abiotic elicitors act synergistically in the induction of phytoalexin accumulation in soybean. Plant Mol Biol **6:** 23–32

De Lorenzo G, Brutus A, Savatin DV, Sicilia F, Cervone F (2011) Engineering plant resistance by constructing chimeric receptors that recognize damage-associated molecular patterns (DAMPs). FEBS Lett **585:** 1521–1528

de Souza A, Hull PA, Gille S, Pauly M (2014) Identification and functional characterization of the distinct plant pectin esterases PAE8 and PAE9 and their deletion mutants. Planta **240:** 1123–1138

De Vos M, Jander G (2009) *Myzus persicae* (green peach aphid) salivary components induce defence responses in *Arabidopsis thaliana*. Plant Cell Environ **32:** 1548–1560

Decreux A, Messiaen J (2005) Wall-associated kinase WAK1 interacts with cell wall pectins in a calcium-induced conformation. Plant Cell Physiol **46:** 268–278

Delaunois B, Jeandet P, Clément C, Baillieul F, Dorey S, Cordelier S (2014) Uncovering plant-pathogen crosstalk through apoplastic proteomic studies. Front Plant Sci **5:** 249

Divol F, Vilaine F, Thibivilliers S, Kusiak C, Sauge MH, Dinant S (2007) Involvement of the xyloglucan endotransglycosylase/hydrolases encoded by celery *XTH1* and Arabidopsis *XTH33* in the phloem response to aphids. Plant Cell Environ **30:** 187–201

Dixon AFG (1973) Biology of Aphids The Institute of Biology, Studies in Biology. Cambridge Rare Books, Cambridge, United Kingdom, pp 1–58

Dreyer DL, Campbell BC (1987) Chemical basis of host plant resistance to aphids. Plant Cell Environ **10:** 553–561

Ferrari S, Savatin DV, Sicilia F, Gramegna G, Cervone F, Lorenzo GD (2013) Oligogalacturonides: Plant damage-associated molecular patterns and regulators of growth and development. Front Plant Sci **4:** 49

Floková K, Tarkowská D, Miersch O, Strnad M, Wasternack C, Novák O (2014) UHPLC-MS/MS based target profiling of stress-induced phytohormones. Phytochemistry **105:** 147–157

Foyer CH, Verrall SR, Hancock RD (2015) Systematic analysis of phloem-feeding insect-induced transcriptional reprogramming in Arabidopsis highlights common features and reveals distinct responses to specialist and generalist insects. J Exp Bot **66:** 495–512

Gao Q-M, Venugopal S, Navarre D, Kachroo A (2011) Low oleic acid-derived repression of jasmonic acid-inducible defense responses requires the WRKY50 and WRKY51 proteins. Plant Physiol **155:** 464–476

Gentleman RC, Carey VJ, Bates DM, Bolstad B, Dettling M, Dudoit S, Ellis B, Gautier L, Ge Y, Gentry J, et al (2004) Bioconductor: Open software development for computational biology and bioinformatics. Genome Biol **5:** R80

Glawischnig E (2007) Camalexin. Phytochemistry **68:** 401–406

Gullberg J, Jonsson P, Nordström A, Sjöström M, Moritz T (2004) Design of experiments: An efficient strategy to identify factors influencing extraction and derivatization of *Arabidopsis thaliana* samples in metabolomic studies with gas chromatography/mass spectrometry. Anal Biochem **331:** 283–295

Hahn MG, Darvill AG, Albersheim P (1981) Host-pathogen interactions: XIX. The endogenous elicitor, a fragment of a plant cell wall polysaccharide that elicits phytoalexin accumulation in soybeans. Plant Physiol **68:** 1161–1169

Heil M, Land WG (2014) Danger signals - damaged-self recognition across the tree of life. Front Plant Sci **5:** 578

Hlavac M (2018) stargazer: Well-Formatted Regression and Summary Statistics Tables. R package version 5.2.2. https://sites.google.com/site/marekhlavac/software/stargazer (January 3, 2019)

Huang H-J, Cui J-R, Xia X, Chen J, Ye Y-X, Zhang C-X, Hong X-Y (2019) Salivary DNase II from *Laodelphax striatellus* acts as an effector that suppresses plant defence. New Phytol **224:** 860–874

Idänheimo N, Gauthier A, Salojärvi J, Siligato R, Brosché M, Kollist H, Mähönen AP, Kangasjärvi J, Wrzaczek M (2014) The *Arabidopsis thaliana* cysteine-rich receptor-like kinases CRK6 and CRK7 protect against apoplastic oxidative stress. Biochem Biophys Res Commun **445:** 457–462

Imbusch R, Mueller MJ (2000) Analysis of oxidative stress and wound-inducible dinor isoprostanes F(1) (phytoprostanes F(1)) in plants. Plant Physiol **124:** 1293–1304

Jambunathan N (2010) Determination and Detection of Reactive Oxygen Species (ROS), Lipid Peroxidation, and Electrolyte Leakage in Plants. In R Sunkar, ed, Plant Stress Tolerance, Methods in Molecular Biology. Springer Science+Business Media, Hatfield, United Kingdom, pp 291–297

Jarvis MC, Apperley DC (1995) Chain conformation in concentrated pectic gels: Evidence from 13C NMR. Carbohydr Res **275:** 131–145

Kärkönen A, Kuchitsu K (2015) Reactive oxygen species in cell wall metabolism and development in plants. Phytochemistry **112:** 22–32

Kettles GJ, Drurey C, Schoonbeek HJ, Maule AJ, Hogenhout SA (2013) Resistance of *Arabidopsis thaliana* to the green peach aphid, *Myzus persicae*, involves camalexin and is regulated by microRNAs. New Phytol **198:** 1178–1190

Kim JH, Lee BW, Schroeder FC, Jander G (2008) Identification of indole glucosinolate breakdown products with antifeedant effects on *Myzus persicae* (green peach aphid). Plant J **54:** 1015–1026

Kloth KJ, Busscher-Lange J, Wiegers GL, Kruijer W, Buijs G, Meyer RC, Albrectsen BR, Bouwmeester HJ, Dicke M, Jongsma MA (2017) SIEVE ELEMENT-LINING CHAPERONE 1 restricts aphid feeding on Arabidopsis during heat stress. Plant Cell **29:** 2450–2464

Kloth KJ, Wiegers GL, Busscher-Lange J, van Haarst JC, Kruijer W, Bouwmeester HJ, Dicke M, Jongsma MA (2016) AtWRKY22 promotes susceptibility to aphids and modulates salicylic acid and jasmonic acid signalling. J Exp Bot **67:** 3383–3396

Kohorn BD, Johansen S, Shishido A, Todorova T, Martinez R, Defeo E, Obregon P (2009) Pectin activation of MAP kinase and gene expression is WAK2 dependent. Plant J **60:** 974–982

Kohorn BD, Kohorn SL, Saba NJ, Martinez VM (2014) Requirement for pectin methyl esterase and preference for fragmented over native pectins for wall-associated kinase-activated, EDS1/PAD4-dependent stress response in Arabidopsis. J Biol Chem **289:** 18978–18986

Kohorn BD, Kohorn SL, Todorova T, Baptiste G, Stansky K, McCullough M (2012) A dominant allele of Arabidopsis pectin-binding wall-associated kinase induces a stress response suppressed by MPK6 but not MPK3 mutations. Mol Plant **5:** 841–851

Kopylova E, Noé L, Touzet H (2012) SortMeRNA: Fast and accurate filtering of ribosomal RNAs in metatranscriptomic data. Bioinformatics **28:** 3211–3217

Kuśnierczyk A, Winge P, Jørstad TS, Troczyńska J, Rossiter JT, Bones AM (2008) Towards global understanding of plant defence against aphids--timing and dynamics of early *Arabidopsis* defence responses to cabbage aphid (*Brevicoryne brassicae*) attack. Plant Cell Environ **31:** 1097–1115

Landry LG, Chapple CC, Last RL (1995) Arabidopsis mutants lacking phenolic sunscreens exhibit enhanced ultraviolet-B injury and oxidative damage. Plant Physiol **109:** 1159–1166

Levesque-Tremblay G, Pelloux J, Braybrook SA, Müller K (2015) Tuning of pectin methylesterification: Consequences for cell wall biomechanics and development. Planta **242:** 791–811

Liners F, Letesson J-J, Didembourg C, Van Cutsem P (1989) Monoclonal antibodies against pectin: recognition of a conformation induced by calcium. Plant Physiol **91:** 1419–1424

Lionetti V, Fabri E, De Caroli M, Hansen AR, Willats WGT, Piro G, Bellincampi D (2017) Three pectin methylesterase inhibitors protect cell wall integrity for Arabidopsis immunity to *Botrytis*. Plant Physiol **173:** 1844–1863

Lotze MT, Zeh HJ, Rubartelli A, Sparvero LJ, Amoscato AA, Washburn NR, Devera ME, Liang X, Tör M, Billiar T (2007) The grateful dead: Damage-associated molecular pattern molecules and reduction/oxidation regulate immunity. Immunol Rev **220:** 60–81

Love MI, Huber W, Anders S (2014) Moderated estimation of fold change and dispersion for RNA-seq data with DESeq2. Genome Biol **15:** 550

Ma R, Reese JC, Black WC, Bramel-Cox P (1990) Detection of pectinesterase and polygalacturonase from salivary secretions of living greenbugs, *Schizaphis graminum* (Homoptera: Aphididae). J Insect Physiol **36:** 507–512

Maere S, Heymans K, Kuiper M (2005) BiNGO: A Cytoscape plugin to assess overrepresentation of gene ontology categories in biological networks. Bioinformatics **21:** 3448–3449

Mao P, Duan M, Wei C, Li Y (2007) WRKY62 transcription factor acts downstream of cytosolic NPR1 and negatively regulates jasmonate-responsive gene expression. Plant Cell Physiol **48:** 833–842

Matzinger P (1994) Tolerance, danger, and the extended family. Annu Rev Immunol **12:** 991–1045

Matzinger P (2002) The danger model: A renewed sense of self. Science **296:** 301–305

McMillan GP, Hedley D, Fyffe L, Pérombelon MCM (1993) Potato resistance to soft-rot erwinias is related to cell wall pectin esterification. Physiol Mol Plant Pathol **42:** 279–289

Mendy B, Wang'ombe MW, Radakovic ZS, Holbein J, Ilyas M, Chopra D, Holton N, Zipfel C, Grundler FMW, Siddique S (2017) Arabidopsis leucine-rich repeat receptor-like kinase NILR1 is required for induction of innate immunity to parasitic nematodes. PLoS Pathog **13:** e1006284

Miles PW (1999) Aphid saliva. Biol Rev Camb Philos Soc **74:** 41–85

Mueller MJ (2004) Archetype signals in plants: The phytoprostanes. Curr Opin Plant Biol **7:** 441–448

Mutti NS, Louis J, Pappan LK, Pappan K, Begum K, Chen M-S, Park Y, Dittmer N, Marshall J, Reese JC, Reeck GR (2008) A protein from the salivary glands of the pea aphid, *Acyrthosiphon pisum*, is essential in feeding on a host plant. Proc Natl Acad Sci USA **105:** 9965–9969

Neilson EH, Goodger JQD, Woodrow IE, Møller BL (2013) Plant chemical defense: At what cost? Trends Plant Sci **18:** 250–258

Nićiforović N, Abramovič H (2014) Sinapic acid and its derivatives: Natural sources and bioactivity. Compr Rev Food Sci Food Saf **13:** 34–51

Novaković L, Guo T, Bacic A, Sampathkumar A, Johnson KL (2018) Hitting the wall-sensing and signaling pathways involved in plant cell wall remodeling in response to abiotic stress. Plants (Basel) **7:** 89

Osorio S, Castillejo C, Quesada MA, Medina-Escobar N, Brownsey GJ, Suau R, Heredia A, Botella MA, Valpuesta V (2008) Partial demethylation of oligogalacturonides by pectin methyl esterase 1 is required for eliciting defence responses in wild strawberry (*Fragaria vesca*). Plant J **54:** 43–55

Pegadaraju V, Louis J, Singh V, Reese JC, Bautor J, Feys BJ, Cook G, Parker JE, Shah J (2007) Phloem-based resistance to green peach aphid is controlled by Arabidopsis *PHYTOALEXIN DEFICIENT4* without its signaling partner *ENHANCED DISEASE SUSCEPTIBILITY1*. Plant J **52:** 332–341

Pelloux J, Rustérucci C, Mellerowicz EJ (2007) New insights into pectin methylesterase structure and function. Trends Plant Sci **12:** 267–277

Pfalz M, Mikkelsen MD, Bednarek P, Olsen CE, Halkier BA, Kroymann J (2011) Metabolic engineering in *Nicotiana benthamiana* reveals key enzyme functions in Arabidopsis indole glucosinolate modification. Plant Cell **23:** 716–729

Philippe F, Pelloux J, Rayon C (2017) Plant pectin acetylesterase structure and function: New insights from bioinformatic analysis. BMC Genomics **18:** 456

Pinheiro J, Bates D, DebRoy S, Sarkar D, R Core Team (2018) Linear and Nonlinear Mixed Effects Models. R package version 3.1-137. https://CRAN.R-project.org/package=nlme (January 3, 2019).

Podgórska A, Burian M, Szal B (2017) Extra-cellular but extra-ordinarily important for cells: Apoplastic reactive oxygen species metabolism. Front Plant Sci **8:** 1353

Pogorelko G, Lionetti V, Bellincampi D, Zabotina O (2013a) Cell wall integrity: Targeted post-synthetic modifications to reveal its role in plant growth and defense against pathogens. Plant Signal Behav **8:** e25435

Pogorelko G, Lionetti V, Fursova O, Sundaram RM, Qi M, Whitham SA, Bogdanove AJ, Bellincampi D, Zabotina OA (2013b) Arabidopsis and *Brachypodium distachyon* transgenic plants expressing *Aspergillus nidulans* acetylesterases have decreased degree of polysaccharide acetylation and increased resistance to pathogens. Plant Physiol **162:** 9–23

R Core Team (2017) R: A Language and Environment for Statistical Computing. R Foundation for Statistical Computing. Vienna, Austria. http://www.R-project.org/ (June 1, 2019)

Raiola A, Lionetti V, Elmaghraby I, Immerzeel P, Mellerowicz EJ, Salvi G, Cervone F, Bellincampi D (2011) Pectin methylesterase is induced in Arabidopsis upon infection and is necessary for a successful colonization by necrotrophic pathogens. Mol Plant Microbe Interact **24:** 432–440

Ridley BL, O'Neill MA, Mohnen D (2001) Pectins: structure, biosynthesis, and oligogalacturonide-related signaling. Phytochemistry **57:** 929–967

Rodriguez PA, Bos JIB (2013) Toward understanding the role of aphid effectors in plant infestation. Mol Plant Microbe Interact **26:** 25–30

Sadhukhan A, Kobayashi Y, Nakano Y, Iuchi S, Kobayashi M, Sahoo L, Koyama H (2017) Genome-wide association study reveals that the aquaporin NIP1;1 contributes to variation in hydrogen peroxide sensitivity in *Arabidopsis thaliana*. Mol Plant **10:** 1082–1094

Schmidt R, Kunkowska AB, Schippers JHM (2016) Role of reactive oxygen species during cell expansion in leaves. Plant Physiol **172:** 2098–2106

Schoonhoven LM, Loon JJA, Dicke M (2005) Insect–plant biology. Oxford University Press, Oxford

Schurch NJ, Schofield P, Gierliński M, Cole C, Sherstnev A, Singh V, Wrobel N, Gharbi K, Simpson GG, Owen-Hughes T, et al (2016) How

many biological replicates are needed in an RNA-seq experiment and which differential expression tool should you use? RNA **22:** 839–851

Schwalb B, Tresch A, Torkler P, Duemcke S, Demel C, Ripley B, Venables B (2018) LSD: Lots of Superior Depictions. R package version 3.0. http://CRAN.R-project.org/package=LSD (February 20, 2018).

Sgherri C, Stevanovic B, Navari-Izzo F (2004) Role of phenolics in the antioxidative status of the resurrection plant Ramonda serbica during dehydration and rehydration. Physiol Plant **122:** 478–485

Shaw SL, Long SR (2003) Nod factor inhibition of reactive oxygen efflux in a host legume. Plant Physiol **132:** 2196–2204

Silva-Sanzana C, Celiz-Balboa J, Garzo E, Marcus SE, Parra-Rojas JP, Rojas B, Olmedo P, Rubilar MA, Rios I, Chorbadjian RA, et al (2019) Pectin methylesterases modulate plant homogalacturonan status in defenses against the aphid *Myzus persicae*. Plant Cell **31:** 1913–1929

Smith CM, Boyko EV (2007) The molecular bases of plant resistance and defense responses to aphid feeding: Current status. Entomol Exp Appl **122:** 1–16

Soneson C, Love M, Robinson M (2015) Differential analyses for RNA-seq: Transcript-level estimates improve gene-level inferences

Stolpe C, Giehren F, Krämer U, Müller C (2017) Both heavy metal-amendment of soil and aphid-infestation increase Cd and Zn concentrations in phloem exudates of a metal-hyperaccumulating plant. Phytochemistry **139:** 109–117

Supek F, Bošnjak M, Škunca N, Šmuc T (2011) REVIGO summarizes and visualizes long lists of gene ontology terms. PLoS One **6:** e21800

ten Broeke CJM, Dicke M, van Loon JJA (2013) Performance and feeding behaviour of two biotypes of the black currant-lettuce aphid, *Nasonovia ribisnigri*, on resistant and susceptible *Lactuca sativa* near-isogenic lines. Bull Entomol Res **103:** 511–521

Tetyuk O, Benning UF, Hoffmann-Benning S (2013) Collection and analysis of Arabidopsis phloem exudates using the EDTA-facilitated Method. J Vis Exp **80:** e51111

Thoma I, Loeffler C, Sinha AK, Gupta M, Krischke M, Steffan B, Roitsch T, Mueller MJ (2003) Cyclopentenone isoprostanes induced by reactive oxygen species trigger defense gene activation and phytoalexin accumulation in plants. Plant J **34:** 363–375

Tjallingii WF (1988) Electrical recording of stylet penetration activities. In AK Minks, and P Harrewijn, eds, Aphids, their biology, natural enemies and control, Vol 2B. Elsevier, Amsterdam, pp 95–108

Tjallingii WF (1994) Sieve element acceptance by aphids. Eur J Entomol **91:** 47–52

Tjallingii WF, Hogen Esch T (1993) Fine structure of aphid stylet routes in plant tissues in correlation with EPG signals. Physiol Entomol **18:** 317–328

Trapalis M, Li SF, Parish RW (2017) The Arabidopsis *GASA10* gene encodes a cell wall protein strongly expressed in developing anthers and seeds. Plant Sci **260:** 71–79

van Bel AJE, Will T (2016) Functional evaluation of proteins in watery and gel saliva of aphids. Front Plant Sci **7:** 1840

Vorhölter F-J, Wiggerich H-G, Scheidle H, Sidhu VK, Mrozek K, Küster H, Pühler A, Niehaus K (2012) Involvement of bacterial TonB-dependent signaling in the generation of an oligogalacturonide damage-associated molecular pattern from plant cell walls exposed to Xanthomonas campestris pv. campestris pectate lyases. BMC Microbiol **12:** 239

Vorwerk S, Somerville S, Somerville C (2004) The role of plant cell wall polysaccharide composition in disease resistance. Trends Plant Sci **9:** 203–209

Wagner TA, Kohorn BD (2001) Wall-associated kinases are expressed throughout plant development and are required for cell expansion. Plant Cell **13:** 303–318

Walker GP, Medina-Ortega KJ (2012) Penetration of faba bean sieve elements by pea aphid does not trigger forisome dispersal. Entomol Exp Appl **144:** 326–335

Waszczak C, Carmody M, Kangasjärvi J (2018) Reactive oxygen species in plant signaling. Annu Rev Plant Biol **69:** 209–236

Willats WGT, McCartney L, Mackie W, Knox JP (2001) Pectin: Cell biology and prospects for functional analysis. Plant Mol Biol **47:** 9–27

Williams KM, Martin WE, Smith J, Williams BS, Garner BL (2012) Production of protocatechuic acid in Bacillus Thuringiensis ATCC33679. Int J Mol Sci **13:** 3765–3772

Wolf S (2017) Plant cell wall signalling and receptor-like kinases. Biochem J **474:** 471–492

Wu J, Baldwin IT (2010) New insights into plant responses to the attack from insect herbivores. Annu Rev Genet **44:** 1–24

Zhang B, Van Aken O, Thatcher L, De Clercq I, Duncan O, Law SR, Murcha MW, van der Merwe M, Seifi HS, Carrie C, et al (2014) The mitochondrial outer membrane AAA ATPase AtOM66 affects cell death and pathogen resistance in Arabidopsis thaliana. Plant J **80:** 709–727

Zhang Y, Talalay P, Cho CG, Posner GH (1992) A major inducer of anticarcinogenic protective enzymes from broccoli: Isolation and elucidation of structure. Proc Natl Acad Sci USA **89:** 2399–2403

Zhou N, Tootle TL, Glazebrook J (1999) Arabidopsis *PAD3*, a gene required for camalexin biosynthesis, encodes a putative cytochrome P450 monooxygenase. Plant Cell **11:** 2419–2428

Zipfel C, Robatzek S, Navarro L, Oakeley EJ, Jones JD, Felix G, Boller T (2004) Bacterial disease resistance in Arabidopsis through flagellin perception. Nature **428:** 764–767